AREA ESTIMATION OF SATELLITE IMAGES USING MACHINE LEARNING ALGORITHMS

A DISSERTATION

Submitted in partial fulfillment of the

requirement for the award of the degree

of

MASTER OF TECHNOLOGY

in

ELECTRICAL ENGINEERING

(With Specialization in Instrumentation and Signal Processing)

By

SANCHIT AGARWAL
(Enrollment No: 17528011)

DEPARTMENT OF ELECTRICAL ENGINEERING
INDIAN INSTITUTE OF TECHNOLOGY
ROORKEE-247667, INDIA
June – 2019

CANDIDATE'S DECLARATION

I hereby certify that this dissertation which is being presented in the progress report titled **"Area Estimation of Satellite Images using Machine Learning "** in partial fulfilment for the requirement of award of Degree of **Master of Technology** in **Electrical Engineering** with specialization in **Instrumentation and Signal Processing**, submitted to the Department of Electrical Engineering, Indian Institute of Technology, Roorkee, India in authentic record of the work carried out during a period from July 2018 to June 2019 under the supervision of **Dr. R.S. Anand** Department of Electrical Engineering, **Dr. Dharmendra Singh** Department of Electronics and Communication Engineering, **Dr. M. Felix Orlando** Department of Electrical Engineering, Indian Institute of Technology Roorkee.

Date:

(SANCHIT AGARWAL)

Place: Roorkee   **Enrollment No: 17528011**

CERTIFICATE

This is to certify that the above statement made by the candidate is correct to the best of my knowledge.

(Dr. R.S. Anand)   **(Dr. Dharmendra Singh)**
Professor   **Professor**
Department of Electrical Engineering   Department of Electronics and Communication Engg.
Indian Institute of Technology   Indian Institute of Technology
Roorkee-247667, India   Roorkee-247667, India

(Dr. M. Felix Orlando)
Assistant Professor
Department of Electrical Engineering
Indian Institute of Technology
Roorkee-247667, India

ACKNOWLEDGEMENT

It is my great pleasure to express my most sincere gratitude and thankfulness to my supervisor Dr. R.S. Anand Electrical Engineering Department, Dr. Dharmendra Singh Electronics and Communication Engineering Department and Dr. M. Felix Orlando Electrical Engineering Department of Indian Institute of Technology, Roorkee, for inspiring guidance, generous help and precious time given throughout this work.

I would also sincerely thank to all my friends, lab members of Microwave Imaging and Space Technology Application Lab (MISTEL) in Electronics and Communication Engineering Department and staff members of IIT Roorkee who have helped me in every possible way in successful completion of my dissertation.

I also take this occasion to thank my family for their help and encouragement in preparing the dissertation.

Place: Roorkee

Date: SANCHIT AGARWAL

TABLE OF CONTENTS

LIST OF FIGURES

LIST OF TABLES

ABSTRACT

Satellites have been used from past several years to obtain a large variety of information about the earth's surface like in military applications, estimating global weather patterns, tectonic activity, surface vegetation, ocean currents and temperature, polar ice fluctuations, pollution, and many other problems. Image acquired from satellites are best choice to extract information regarding the natural resources of country that can be extremely useful for planning purposes. Resources include agricultural, geological and strategic resources. Such information can be conveniently extracted from satellite images with application of suitable digital image processing techniques. The low and high level computation using machine learning algorithms can be done for earth's surface using satellite images. The main emphasis of this thesis is using various machine learning algorithms for area estimation with satellite images for five different classes namely soil, urban, water, vegetation and dark forest regions, spectral unmixing for mixed pixels for calculation of fractional vegetation cover, using different type of vegetation and built-up indices and also calculation textural features such as mean, entropy and roughness for proper classification of soil and urban region in optical satellite images. The study and techniques applied have been performed on region of Uttarakhand, India i.e. Roorkee city and surrounding area.

CHAPTER 1

INTRODUCTION

There are several satellite images available with different spatial resolutions and spectral characteristics. Resolution describes the smallest unit in satellite image is single pixel describing the area on Earth's surface represented by that particular pixel. High spatial resolution satellite data have spatial resolution from 50 centimeters to 100 meters. These data are suitable for variety of applications involving mapping, monitoring, and area estimation of land cover and land use features such as agricultural and urban planning, cartography, climatology, oceanography, military surveillance and infrastructure mapping and many others. Sentinel-2, Landsat 8 are few examples of satellite that offer high spatial resolution of 10-60 meters. On the other hand, low resolution satellite images are also available with advantage of higher temporal resolution (i.e. daily to several times per day coverage). These data are useful for surface temperature monitoring, fire monitoring, regional vegetation and draught studies. Examples of low resolution satellite images include NOAA/AVHRR and MODIS with spatial resolution of 1.1 km and 250-1000 meters respectively. Most of satellite image analysis based algorithms employ high resolution satellite data offer limited spatial coverage and revisit frequency, resulting in strong limitation of acquiring cloud free images.

A few researchers have proposed satellite images analysis based solutions for area estimation of satellite images using machine learning algorithms. There are several advanced machine intelligence and soft computing techniques available i.e. fuzzy logic, Support Vector Machines, K-means, Principal Component Analysis, Neural Networks, which offer significant advantages and are being used extensively by many researchers. For example, fuzzy logic can handle uncertain information, SVM and Neural Networks can provide more accurate classification, K-means can be applied to new unknown region for appropriate classification and PCA can reduce the input feature dimensions without compromising the system performance. Several algorithms exist which utilize the potential application of these techniques quite effectively for different satellite imaging applications.

Satellite images come with different number of spectral channels where each channel has its own significance and is suitable for particular application. For example, visible and near-infrared channels are quite suitable for cloud, water and agriculture monitoring, whereas, thermal channels are useful for monitoring sea surface temperature, forest fires and many other applications. In addition to the spectral channels, other indices, for example NDVI can also give significant contribution for developing solutions for particular problem. Therefore, the statistical information extracted from the combinations of these bands, by employing suitable DIP techniques, may be quite effective in developing a mathematical model for area estimation.

1.1 Motivation and Scope

Farms provide food for us, we take oxygen and building materials from forests, rivers and lakes provide us fresh water to drink, and we live in cities. The exhaustive description of land and water cover

alteration on earth can be found through proper terrain classification. Remote sensing shows a significant part in ground classification. Several classification algorithms have previously been proposed, but further development is required. The incentive behind taking up the task of land and water classification through optical data and applying various Ensemble learning approaches for mixed pixel classification which takes less time and easy to understand for human being as compare to Artificial neural network techniques.

1.2 Aim and Objective

1.2.1 Aim

The present work aims to utilize freely available high resolution satellite data for providing fully adaptive, economical, and promising solution to problem of area estimation. Furthermore, objectives of this project is to explore the applicability of image processing techniques, to provide novel features, and to apply machine intelligence algorithms for devising simple, adaptive and efficient algorithms. Key challenges and issues inherent in development of algorithms include:

- Inaccurate calibration and georeferencing may result in wrong predictions and conclusions.
- Presence of cloud, water and noisy pixels may produce false alarms.
- It is very difficult to observe anything in satellite images acquired in visible spectrum and in order to extract the desired information from basic image processing techniques, advanced techniques need to be developed which take into account the information of multi-spectral bands.
- In a multi-spectral satellite image, the information represented by each band is different than other bands and therefore each band has its own significance for different applications. Hence, in order to find out the desired result, it is very important to analyze the importance of each band and then exploit the information of only appropriate bands to develop the solution.

1.2.2 Objective

The main objective of this dissertation is to estimate area of different land cover with satellite images using machine learning algorithms which contains different tasks that were performed in order to accomplish the goal are:

- Calculating Hough Transform, Otsu segmentation, and bilateral filter techniques for edge detection of the satellite images.
- Generating mask of different classes to be applied for classification of satellite images.
- Applying numerous supervised techniques (Minimum distance, Maximum likelihood) and unsupervised techniques (K-means and ISOdata) for classification of satellite image into 5 distinguished classes namely: Forest, Vegetation, Urban, Water, Barren land.
- Calculation of area of various classes by pixel counting.
- Measure the accuracy for classification of 5 classes using confusion matrix.

- Comparing results of Ensemble learning approach and Back propagation algorithm for mixed pixel classification.
- Computing Fractional Vegetation cover using linear sub pixel analysis model.
- Calculating different Vegetation Indices and textural features for classifying urban and soil that are having almost similar reflectance values.

1.3 Organization of thesis

The thesis consists of five chapters:

In chapter 1, contains introduction of dissertation.

In chapter 2, discussed about basics of area estimation of satellite images, various mathematical formulae used for calculation and classification.

In chapter 3, tells about study data and various preprocessing done for satellite images. It also discusses about the various methodologies used in this dissertation

In chapter 4, results of all the classification techniques are explain and compare with the help of confusion matrix.

Chapter 5 summarizes the obtained results with concluding remarks.

CHAPTER 2

BRIEF REVIEW

In this chapter various classification algorithm techniques have been discussed for calculation of Area. It also discusses various formulas used for classifying data.

2.1 Area Estimation of Agricultural Fields

Area estimation of agricultural fields is used to estimate the area of an agricultural field according to agricultural subsidy system. Income subsidy can be applied by farmers using these, Type and acreage decides their height. Sometimes a farmer either intentionally or non-intentionally overestimates the area, for example by including the surrounding ditches. For saving the worth on incorrect application, correct subsidy must be used to check it. For this, correct area estimation is obtained by each crop. To save from cheatings the field area estimation can also be used for money saving. For easy are estimation a forecast per crop can be done. According to this forecast, the height of the subsidy and spend money can be calculated. So, correct area estimation of an agricultural field is compulsory. Since each remotely sensed image occupies big area, many claims can be observed in relatively cost-effective way, then inspector visits these marked possible cheating areas only that is final. Further, observation can be performed continuously because the satellite passes over the same area regularly. Automated system based on satellite remote sensing is perfectly suitable for crop area estimation.

2.2 Satellite data

Remote sensing is used for taking information about Earth surface and using Electromagnetic spectrum by taking reflected and emitted rays. The best source of radiation is Sun which has full range of EM spectrum. Artificial source of electromagnetic radiation are also used commonly known as active remote sensing. Radiation on reaching the earth, its different parts are reflected, absorbed and emitted mainly in form of thermal energy depending upon the wavelength and material properties. Spectral reflectance curves of materials such as vegetation, soil can be calculated by knowing its electromagnetic energy reflected and absorbed. Two types of passive image scanners namely mechanical and push broom scanner are available on satellite to calculate different reflected and emitted radiation.

Table 2.1 Principal divisions of the electromagnetic spectrum

Division	Wavelength
Gamma rays	< 0.03 nm
X-rays	0.03-3 nm
Ultraviolet	3-380 nm
Blue	0.4-0.5 μm
Green	0.5-0.6 μm
Red	0.6-0.7 μm
Near Infrared	0.72-1.3 μm
Mid Infrared	1.3-3 μm
Far Infrared	3-1000 μm
Microwave	0.1-30 cm
Radio	≥ 30 cm

2.2.1 Microwave

Remote sensing is target properties on the surface of Earth without physical contact [1]. Usually data is required from aircraft or satellite. It is noticed that the microwave band gives important information about targets on the Earth. Microwaves can be used to observe in any climate because of its penetration power and can works in dark and light to measure soil moisture. Microwaves are sensitive to dielectric properties of target, surface roughness and objects that are made by people. Microwave remote sensing is of two types namely active and passive. Active consist a self-illuminated sensor and passive consist sensors records naturally emitted microwave radiation from objects.

Imaging radar has some application areas as follows-
• Observation of ocean.
• Monitoring of Snow and ice, use of land, forest and crops etc. and flood.
• Studying soil moisture, wetlands and the surface movements caused by earthquakes and glacier advancement.

2.2.2 Optical

The sensors function of this part includes visible, near infrared and short-wave infrared wavelengths [1]. These wavelengths are needed for discrimination between forest types and other vegetation classes. Usually satellite sensors are used for detailed mapping include SPOT, Landsat, and Sentinel-2 with moderate resolution (pixel size 10 to 30 m).

Optical satellite data can be combined with laser data because the colour information in optical satellite data can distinguish different vegetation types while laser data provides additional information about terrain or vegetation characteristics. For example, a current application with Sentinel-2 data – which

acquires a new image over a given area in every 3 days at northern latitudes, and has more bands in the "red edge" wavelength region – is to classify and map tree species.

Optical remote sensors detects the solar radiation reflected from targets on the Earth's surface for images by using visible, near infrared and short-wave infrared sensors. Various materials reflect and absorb various wavelengths. So, the targets can be discriminated by their spectral reflectance signatures using remotely sensed images. Based on number of spectral bands that are used in the imaging process, it can be classified into four parts.

- **Panchromatic imaging system**: It is single channel detector that is sensitive to radiation within a broad wavelength range. If the wavelength range is over the visible range, then image will be "black-and-white" that means spectral information or "colour" of the targets is lost.. Brightness of the targets is the measurable physical quantity. For examples IKONOS PAN and SPOT HRV-PAN [1].

- **Multispectral imaging system**: It is multichannel detector with a few spectral bands. It is sensitive to radiation within a narrow wavelength band. Multilayer resulted image has brightness and spectral (colour) information. For examples LANDSAT MSS, LANDSAT TM, SPOT HRV-XS and IKONOS MS [1].

- **Superspectral Imaging System**: It has several spectral channels (typically >10) than others. The bands have narrow bandwidths that gives fine spectral characteristics. For examples MODIS and MERIS [1].

- **Hyperspectral Imaging System**: It is also known as an "imaging spectrometer".It requires images in about a hundred or more contiguous spectral bands. The precise spectral information gives more characterization and identification of objects. These have potential applications like precision agriculture (e.g. monitoring the types, health, moisture status and maturity of crops), management of coastal (e.g. monitoring of phytoplankton's, pollution, bathymetry changes). For example Hyperion on EO1 satellite [1].
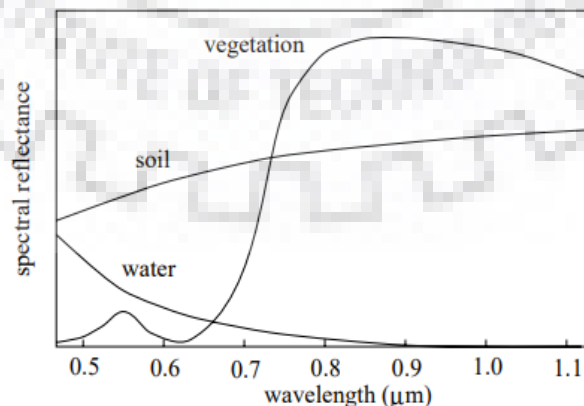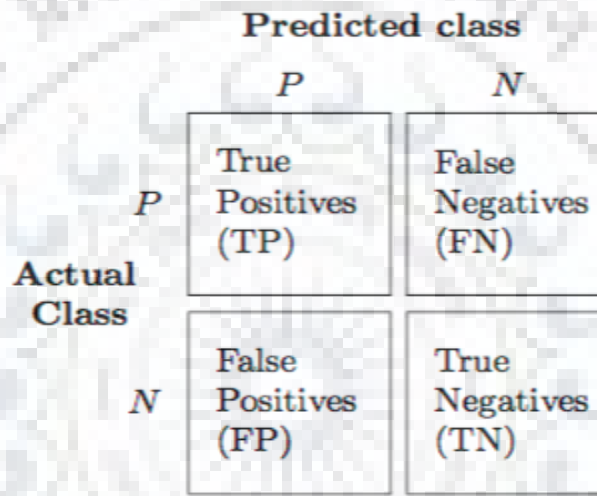
Figure 2.1 Generalized spectral reflectance curves for three different materials [1]

2.3 Mathematical Formulae applied

2.3.1 Confusion Matrix

It is used to merge the performance of classification algorithms. Classification accuracy can be misguiding due to unequal number of observations or due to more classes present. Confusion matrix provides the knowledge of correct classification model and errors that occur in it.

Each row and column denotes instances in a predicted class and actual class respectively. It is a contingency table (table that displays frequency distribution of variables including actual and predicted dimensions [2].

	Predicted class	
	P	N
Actual Class — P	True Positives (TP)	False Negatives (FN)
Actual Class — N	False Positives (FP)	True Negatives (TN)

Figure 2.2 Confusion Matrix [3]

$$Producer\ accuracy = \frac{TP}{TP + FP} \tag{1}$$

$$User\ accuracy = \frac{TP}{TP + FN} \tag{2}$$

$$Sensitivity(S_n) = \frac{TP}{TP + FN} \tag{3}$$

$$Specificity(S_p) = \frac{TN}{TN + FP} \tag{4}$$

Where TP (True Positive) and TN (True Negative) refer to positive pixels correctly classified as positive, and negative pixels correctly classified as negative by the algorithm, respectively. Similarly, FP(False Positive) and FN(False Negative) represent negative pixels falsely classified/ misclassified as positive, and positive pixels is classified as negative by the algorithm, respectively. It is to be noted that

positive denotes one land cover class and negative denotes as other class. It is also noting that terms 'sensitivity of soil' and 'specificity of urban' are used interchangeably.

2.3.2 Separability Index

Since only two classes urban and soil are there for separation, Separability Index (SI) is used to determine whether particular textural or index parameter used will be able to separate two classes or not [4]. It is computed using the following equation 5:

$$SI = \frac{\mu_1 - \mu_2}{\sigma_1 + \sigma_2} \qquad (5)$$

μ_1 and μ_2 are the means, and σ_1 and σ_2 are the standard deviations of the two classes present. Low values of SI i.e. less than 1 implies that particular method used is not effective for classification of 2 classes(Urban and Soil).The value of SI higher than 1 has effective result for classification of 2 classes. SI greater than 1.5 indicates accuracy greater than 90%.

2.4 Literature Review

Mapping and area estimation are complementary objectives, they are closely related but used for different needs and give distinct priorities to distinct precise measurements. Area estimation has a more direct economic effect and very early found a user community with clearly defined precise specifications that are used in agriculture or forest.

Supervised and Unsupervised learning algorithms are used to categorize the land cover data into five sub classes based on spectral basis. K-means [5] and ISOdata [6] algorithm used to categorize by forming clusters of pixel values. Minimum Distance and Mahalanobis distance [2] classifier calculates Euclidean distance of pixel from the mean of the training pixel values and assign the pixels into subsequent classes. Maximum likelihood classifier computes the probability density function and uses Baye's probability by assigning pixel to the class having highest probability. Support Vector Machines [2] uses hyperplanes to classify between different classes. It uses different type of kernels like sigmoid function for non-linear classification techniques. The accuracy of these classifications techniques is further improved by using better approaches for mixed pixel analysis.

Ensemble approach uses the mixed pixels and targets on their classification using the texture feature [7]. Reason to use of it is that texture depends on the spatial arrangement of intensities of an image. Problem of mixed pixels are solved by texture features like colour intensity, energy and local binary pattern [8]. Supervised learning techniques like artificial neural network and ensemble learning are used and for better resolution and to handle the mixed pixel issue, these are compared. Textural information is also used for extracting useful information of targets. While analysing natural targets like tall vegetation, characteristic of textural feature [4] as roughness, may be an important parameter which could identify these targets, since both the classes possess different types of roughness [9]-[10].

Fractional green vegetation cover (FVC) is needed for several environmental and climate related applications [11]. Idea behind estimation, FVC consists linear unmixing of two spectral endmembers as bare soil and green vegetation [12]. The spectral properties are calculated that depends on field measurements, estimated using additional data sources (example soil databases or land cover maps) or extracted directly from the imagery [13]. Linear Spectral unmixing model [13] uses reflectance values of soil and vegetation to segregate them by using pure pixel reflectance value as endmembers and calculating fractional cover of that mixed pixel.

Several built-up and radiometric indices are used to distinguish urban and soil [14]-[16]. Because of its simplicity and easy implementation it broadly used for urban growth monitoring [17]. In literature, it is shown that built-up indices depends on image resolution, seasonality, and study area location [18] and most of them confuse urban with soil and land [19].

Texture refers to the degree of surface roughness or homogeneity of an area of the image. It defines the spatial distribution of image intensity for a given scene category, it enables to use of textural features for objects classification [4]. It distributes structural elements within vegetation or urban and land cover. Thus, it is necessary to produce a precise textural features that consists nearby information of pixel that is further used to distinguish soil and urban.

CHAPTER 3

METHODOLOGY

Satellite Image Processing is a method to enhance raw images received from cameras or sensors placed on satellites, space probes and aircrafts.Satellite image is taken from Sentinel-2 data. First of all preprocessing of satellite image is done before applying image processing techniques. Supervised and Unsupervised classification techniques are applied to classify the land cover into five classes as soil, urban, forest, water and vegetation. The results of these classifications have been improved using Ensemble approach and Backpropagation algorithm. Areas of these classes are calculated using pixel counting. Fractional Vegetation cover for whole area is calculated using spectral mixture analysis by considering soil and vegetation as endmembers. It calculates the vegetation area considering fractional part of the pixel. The reflectance of soil and urban is almost same, so it is difficult to classify using former classification techniques. Radiometric indices and Textural features are used to segregate into two classes.

3.1 Study Area and data set used

3.1.1 Study Area

The study of satellite data was done in surrounding areas of Roorkee, Uttarakhand (India). The study area lies between latitude 29.43^0 N and 30.027^0 N and longitudes 77.54^0 E and 78.11^0 E. The land cover of study area is fairly flat, also contain some mountain regions and mainly consist of urban, water and agriculture classes. The major water bodies are Solani River and Upper Ganga Canal. The key urban areas besides small villages are Roorkee and Haridwar city throughout the study site. Google Earth image of study area has been shown in Figure 3.1 marking different classes namely soil, water, urban, vegetation and forest.

Figure 3.1 Google Earth image of Study Area

3.1.2 Data set used

Sentinel-2 consists of 2 satellites namely Sentinel-2A and Sentinel-2B which are equipped with Multispectral Instruments (MSI) that are capable of getting information from 13 bands at different spatial resolutions (10m, 20m and 60 m) with 10 days revisit time. Sentinel-2 gives more details in NIR band range and SWIR band which are helpful in applications like agriculture, forest monitoring, and natural disaster management. A drawback of Sentinel-2 is no thermal infrared bands are present. Quality of spectral image is determined by number of band and spatial and temporal resolution making Sentinel-2 satellite more suitable for remote sensing applications. Sentinel-2 data has an advantage of free availability of data. Besides this it has software SNAP which is specially designed for processing Sentinel data. ENVI software is also helpful for getting information from the satellite images [20]. Sentinel-2 images of test site is shown for various dates has been taken which has been shown with the Data ID of that image in the Table 3.1. Sentinel-2 image is shown in Figure 3.2.
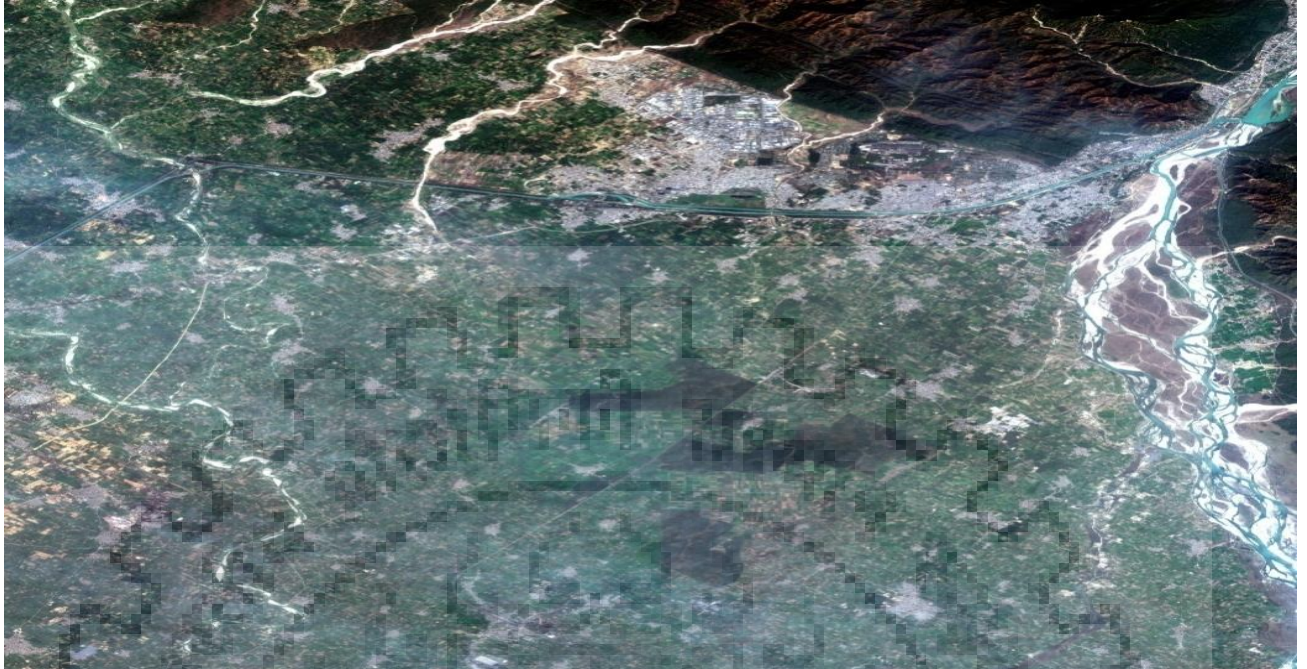
Figure 3.2 Sentinel-2 RGB (Red- Band 4, Green- Band 3, Blue- Band 4) image

Table 3.1 Sentinel-2 images of different dates with data id

Sentinel-2 image	Data ID	Data Id No.
25 April 2019	S2B_MSIL2A_20190425T052649_NO211_RT105_T43RGP_20190425T094130	1
15 April 2019	S2B_MSIL2A_20190415T052649_NO211_RT105_T43RGP_20190415T094430	2
14 February 2018	S2B_MSIL2A_20180214T052649_NO208_RT105_T43RGP_20180214T073425	3
22 October 2017	S2B_MSIL2A_20171022T052839_NO205_RT105_T43RGP_20171022T053409	4
7 October 2017	S2B_MSIL2A_20171007T052711_NO211_RT105_T43RGP_20171007T053044	5
10 April 2017	S2B_MSIL2A_20170410T052641_NO204_RT105_T43RGP_20170410T053057	6
11 December 2016	S2B_MSIL2A_20161211T053222_NO204_RT105_T43RGP_20161211T053220	7

3.1.3 Software Used

During the dissertation work mainly four software's are used:

- **ENVI 5.1** - Environment for Visualizing Images (ENVI) was used for classification of satellite images, calculating region of interest, development of decision tree classification algorithm and calculation of confusion matrix.

- **MATLAB 2018**- This software was used for calculation of Euclidean distance, Fractional vegetation cover, Separability index and using sliding window for Textural features.

- **SNAP-**It is a software used for Sentinel-2 images. Preprocessing of data like resampling, subset selection and atmospheric correction is done in this tool. Various vegetation indices like NDVI, SAVI, BAEI etc. have been calculated using this software.

3.2 Preprocessing of Sentinel-2 image

The preprocessing of satellite images have to be done before applying any further techniques on it which include Resampling of data, Atmospheric Correction and Subset selection. Resampling of image is done so that each band of satellite has same resolution and same number of pixels. Subset selection is performed to choose our area of interest in particular satellite image. It is also done to choose that what bands we have to use out of total bands in that image. Atmospheric Correction algorithms are based on the Atmospheric/Topographic Correction for Satellite.

Richter method has performed atmospheric correction using libRadtran radiative transfer model [21] which generates look up tables for various atmospheric conditions, solar geometries and ground elevations. This model is computes the bottom-of-atmosphere reflectance values. Thus all gaseous properties vapor content, aerosol thickness and aerosol properties of the atmosphere are calculated. Sen2Cor is plugin provided inside SNAP for making atmospheric corrections. The bands of Sentinel-2 image are shown in Table 3.2 with their wavelength and resolutions.

Table 3.2 Bands of Sentinel-2 satellite [22]

Sentinel-2 bands	Central Wavelength (µm)	Resolution (m)
Band 1- Coastal aerosol	0.443	60
Band 2- Blue	0.490	10
Band 3- Green	0.560	10
Band 4- Red	0.665	10
Band 5- Near Infrared	0.705	20
Band 6- Near Infrared	0.740	20
Band 7- Near Infrared	0.783	20
Band 8- Near Infrared	0.842	10
Band 8A- Near Infrared	0.865	20
Band 9- Water Vapour	0.945	60
Band 10- Shortwave Infrared (Cirrus)	1.375	60
Band 11- Shortwave Infrared	1.610	20
Band 12- Shortwave Infrared	2.190	20

3.3 Masking Technique

To apply classification on satellite image various masks of different classes are created individually. The mask of different classes can be created using different band characteristics. Different bands used for Sentinel 2 image are Red, Blue, Green, NIR (Near Infrared). Water mask are created using NIR and Red band. Forest and Vegetation mask is created using NIR and Green band. Urban mask is created using Red and Green band. Barren land mask is created using Red, Green and Blue band. To create mask we collect the reflectance range of particular class in different bands. After masking of different classes assignment of different colors is given to particular class. Water is given dark blue, Forest is given dark green, Vegetation is given light green, Urban region is given red color and Barren land is given yellow color. For particular mask '0' means white which tells about the given class whereas '255' means black which is the rest region. Flowchart for masking is shown in Figure 3.3. Masking technique used is the preliminary data interpretation of pixels in satellite image.

Input sentinel -2

Resampling and subset of image is done by taking red, green, blue and Near Infrared (NIR) bands

Region of interest for 5 different classes namely soil, urban, vegetation, forest and water are calculated.

Range of reflectance values of bands are taken for all the 5 different classes

Masking of all the classes is done considering the range of reflectance values with exhaustive analysis

Classified image is calculated by combining different masks and assigning various colour to different classes

Figure 3.3 Flowchart for masking

3.4 Unsupervised and Supervised Classification

Classification is defined for particular pixel or spatially combined sets of pixels which represents some feature, class, or material that are described by a range of digital numbers or reflectance values for each band. There are two methods of classification namely unsupervised and supervised classification [1] as show in Figure 3.4
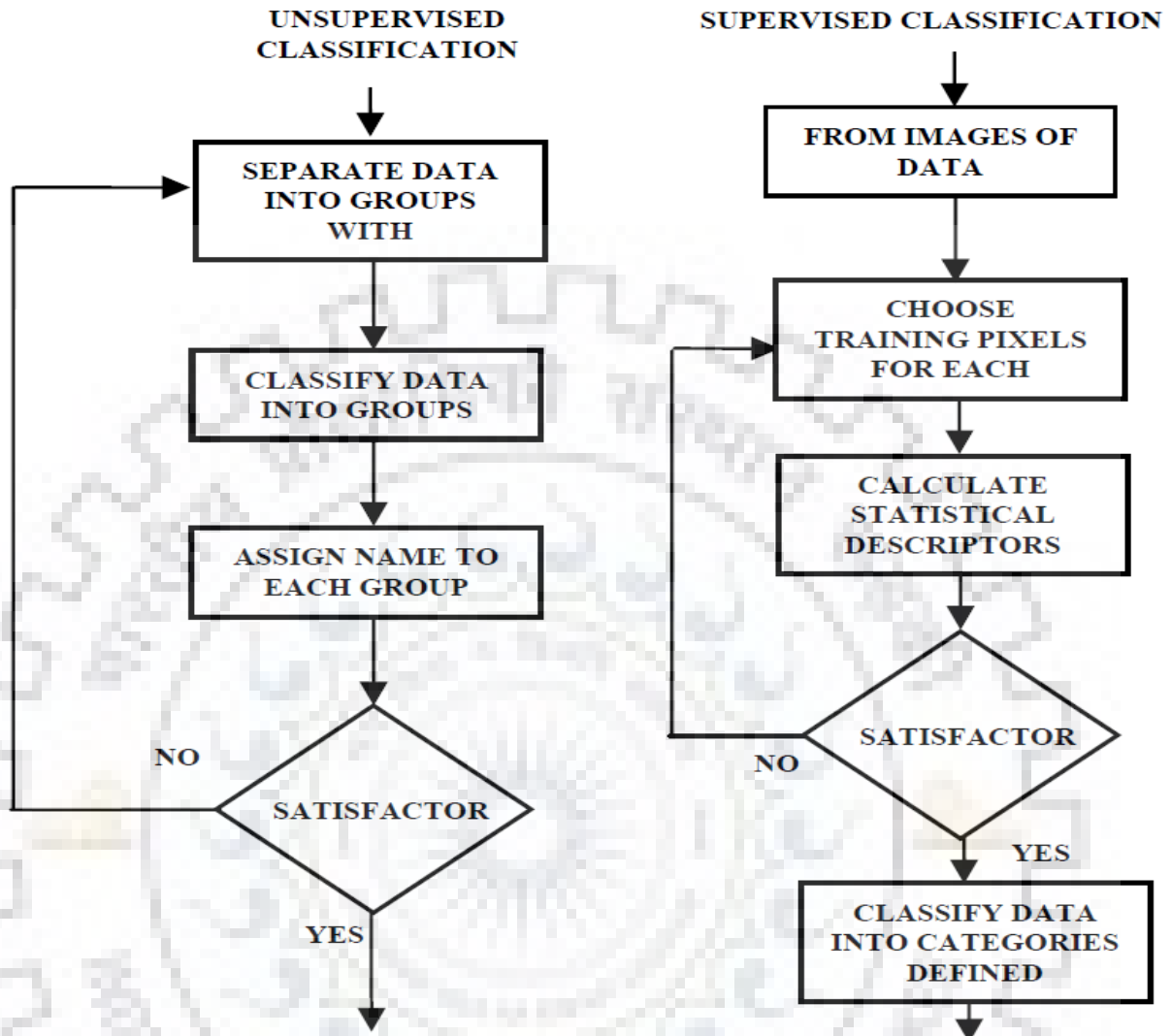
Figure 3.4 Flowchart of supervised and unsupervised classification [1]

3.4.1 Unsupervised Classification

In unsupervised classification, each pixel is compared to each discrete cluster to find nearer pixel. Clusters are statistically separable in the group of multiband spectral response patterns. Segregation of different classes depends upon the parameters we choose. Unsupervised classification is used to classify the data without prior knowledge of the image.

3.4.1.1 ISOdata (Iterative Self-Organizing) Classifier [6]

Iterative Self-Organizing Data (ISOdata) adjusts number of clusters automatically when iteration goes on by merging similar clusters and splitting clusters [6]. Merging is done when number of members (pixel) in a cluster is lesser than a particular threshold or mean of two clusters are closer than a certain threshold.

Splitting is done when standard deviation of cluster greater than predefined value and the number of members (pixels) is double of threshold for the minimum number of members.

This algorithm is same as k-means algorithm except ISOdata allows number of cluster while number of clusters should be known in k-means.

- Each pixel is compared to each cluster mean and put into the cluster whose mean is closest in Euclidean distance.

$$\sqrt{\left(D_{B1j} - D_{B1\mu}\right)^2 + ... + \left(D_{Bnj} - D_{Bn\mu}\right)^2} \tag{6}$$

Where

D_{Bij} = digital number of cluster where $i = (0, n)$

$D_{Bi\mu}$ = digital number of mean cluster where $i = (0, n)$

- Center of new cluster is calculated by taking mean of the pixels in that cluster.
- Sum of Squared Errors (SSE) finds the cumulative squared difference for distinct bands of each pixel from the center for each cluster individually, and then adds them.
- ISOdata algorithm stops either any iteration threshold is achieved or the maximum percentage of unchanged pixel threshold is achieved.

3.4.1.2 K-Means

K-means algorithm allows a simplest way of classifying a given data set through a fixed certain number of clusters (k) [23]. Idea of this algorithm is to define centroid for each cluster that placed in cunning way (far away to each other) because distinct location is for distinct result then associate each point to the nearest centroid. So, k new centroids are got, a new binding has to be done between the same data set points and the nearest new centroid. A loop has been generated and it is observed that k centroids don't change location until no more changes are done. This algorithm minimizes squared error function [5].

K-means algorithm has following three steps that iterate until stable -

- Determine the centroid for each cluster.
- Compute the distance of each cluster form centroid.
- Group the cluster based on minimum distance.

After doing these steps, segmentation and classification results are stored and given to NN (neural network) for further segmentation and classification.

3.4.2 Supervised Classification

In supervised classification, classes are known that present within the scene. In multiband data, statistical analysis is used for different classes. Pixels that are outside the training sites are compared class discriminates, if it is nearer then map of established classes.

3.4.2.1 Parallelepiped Classifier

It is also called multi-level slicing that divides each axis of multi-spectral feature space [2], as shown in Figure 3.5.
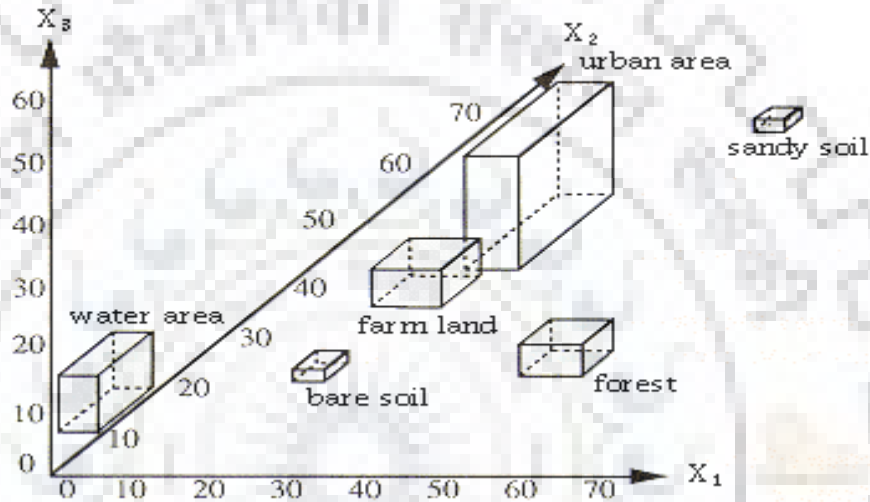
Figure 3.5 Schematic concept of parallel piped classifier in three dimensional feature spaces [2]

The decision region is determined by minimum and maximum values on each axis after considering the population statistics those results of accuracy. For two-dimensional, it forms a rectangular. Number of boxes form for number of classes.

3.4.2.2 Mahalanobis Distance

It measures the distance between a point (P) and a distribution (D). Idea of this multi-dimensional generalization to calculate how many standard deviations (P) are far away from the mean of (D). If distance point (P) and mean distance (D) are at same place then distance is zero and if P moves away from the mean then distance increases along each principal component axis, Number of standard deviations are measured by Mahalanobis distance from P to the mean of D [2]. If each axes are rescaled to get variance as unity then the Mahalanobis distance represents standard Euclidean distance in the transformed space. Consequently the Mahalanobis distance has no units and scale invariant, and takes into account the correlations of the data set.

$$D_M(\vec{x}) = \sqrt{(\vec{x} - \vec{\mu})^T s^{-1} (\vec{x} - \vec{\mu})} \tag{7}$$

$$d(\vec{x}, \vec{y}) = \sqrt{(\vec{x} - \vec{y})^T s^{-1} (\vec{x} - \vec{y})} \tag{8}$$

$$Mahalanobis\ distance = \vec{x} = (x_1, x_2, \dots, x_N)^T \tag{9}$$

$$Mean\ distance = \vec{\mu} = (\mu_1, \mu_2, \dots, \mu_N)^T \tag{10}$$

$$S = covariance\ matrix$$

Probability contours is used to define the Mahalanobis distance. The Mahalanobis distance has the following properties:

- Different variances in various direction.
- It removes the covariance that is present between the variables.
- It reduces to Euclidean distance for non-correlated variables with unit variance.

Univariate z-score standardizes the distribution (for zero mean and unit variance) for univariate normal data and gives a dimensionless quantity that specifies the distance from an observation to the mean in terms of the scale of the data. Mahalanobis distance calculates the Euclidean distance on the uncorrelated data by computing the variance and covariance between variables.

3.4.2.3 Minimum Distance Classifier

It is referred as central and simplest classifier.

- Determination of mean of each training class.
- Calculation of Euclidean distance from the mean for each pixel.
- Assign pixel that has minimum Euclidean distance to the mean.

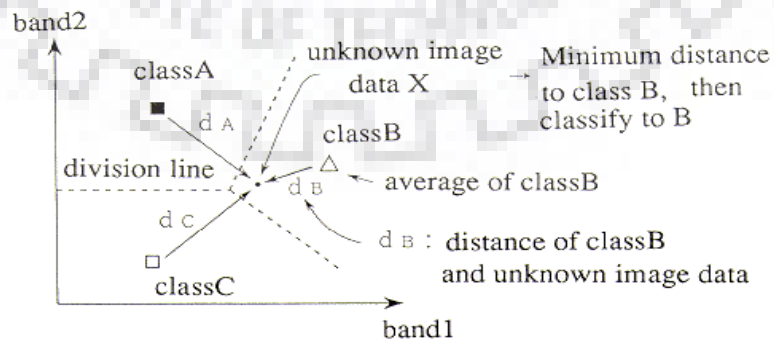Figure 3.6 shows the concept of a minimum distance classifier.

Figure 3.6 Minimum Distance classifier [2]

Unknown pixels are classified to the class which has minimum distance between the image data and the class in multi feature space. In the Euclidean plane,

$$a = (a_1, a_2) \tag{11}$$

$$b = (b_1, b_2) \tag{12}$$

$$d(a, b) = \sqrt{(a_1 - b_1)^2 + (a_2 - b_2)^2} \tag{13}$$

3.4.2.4 Support Vector Machine (SVM)

SVM defines the decision planes (hyper planes) that are used to separate objects having different classes. Minimum distance of training samples is given by hyperplane. Hyperplane gives large margin that has the maximum distance to the closest training data that gives good separation. Support Vectors are the margin pushes up against [2]. Hyperplane image of Support Vector Machine classifier is shown in Figure 3.7.

Figure 3.7 Hyperplane image of SVM [2]
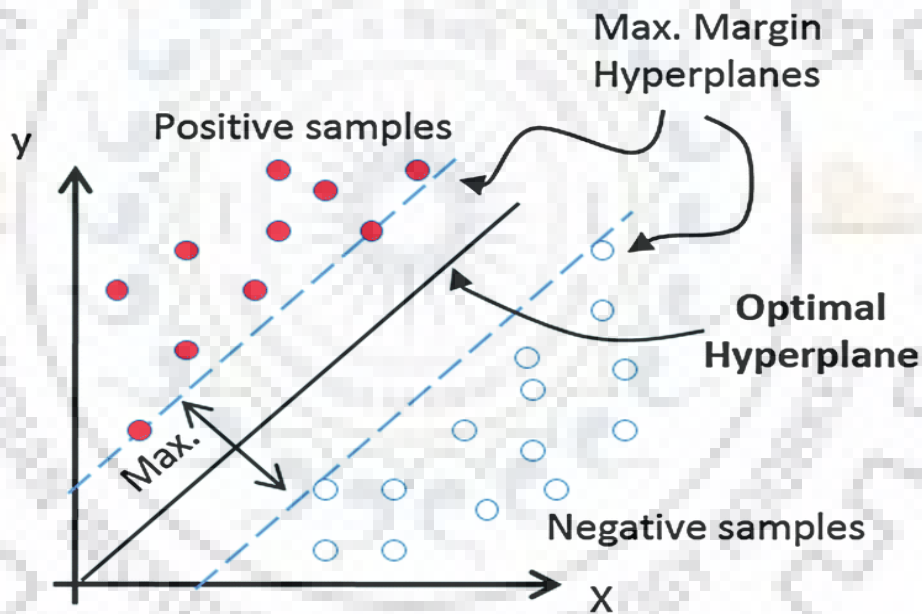
The hyperplane is generally expressed by weights W and bias B (any real number), X corresponds to the data values. SVM usually maximizes the margin between data values of opposite classes.

$$W.X + B = 0 \tag{14}$$

The original hyperplane constructs a linear classifier. Various Kernel functions are used for nonlinear classifiers.

$$K(x_i, x_j) = \phi(x_i).\phi(x_j) \tag{15}$$

There are many models to use with kernel functions of them:

- The Linear Kernel

$$K(x_i, x_j) = x_i . x_j \qquad (16)$$

- The polynomial kernel of order p

$$K(x_i, x_j) = (1 + x_i . x_j)^p \qquad (17)$$

- The radial basis function kernel

$$K(x_i, x_j) = exp\left[-\frac{(x_i - x_j)(x_i - x_j)}{2\sigma^2}\right] \qquad (18)$$

- The sigmoid kernel

$$K(x_i, x_j) = exp\left[\frac{1}{1 + exp[\beta_o x_i . x_j + \beta_1]}\right] \qquad (19)$$

3.4.2.5 Maximum Likelihood Classifier (MLE)

It classifies a pixel into respective classes using maximum likelihood. Likelihood (L_k) is defined as the posterior probability of a pixel belonging to class k [2],

$$L_k = P(k) * \frac{P\left(\frac{X}{k}\right)}{P(i)P\left(\frac{X}{i}\right)} \qquad (20)$$

$P(k)$: Prior probability of class k

$P\left(\frac{X}{k}\right)$: Conditional probability to observe X from class k, or probability density function

Normally prior probabilities are assumed to be same and P(i)*P(X/i) is also same for all classes. Thus likelihood depends on the probability density function. For mathematical reasons, a multivariate normal distribution is given as the probability density function. Formula for Likelihood can be given as follows-

$$L_k(X) = \frac{1}{\sqrt{(2)^n |\Sigma_k|}} e^{\left(-\frac{1}{2}\right)(X - X_k)^T (\Sigma)^{-1}(X - x_k)} \qquad (21)$$

where,

n: number of bands
X: image data of n bands
L_k (X) : likelihood of X belonging to class k
X_k : mean vector of class k
Σ_k: variance-covariance matrix of class k
$|\Sigma_k|$:is determinant of $|\Sigma_k|$:

When the variance-covariance matrix is symmetric, the likelihood is the same as the Euclidian distance. Probability density graph for Maximum likelihood classifier is shown in Figure 3.8
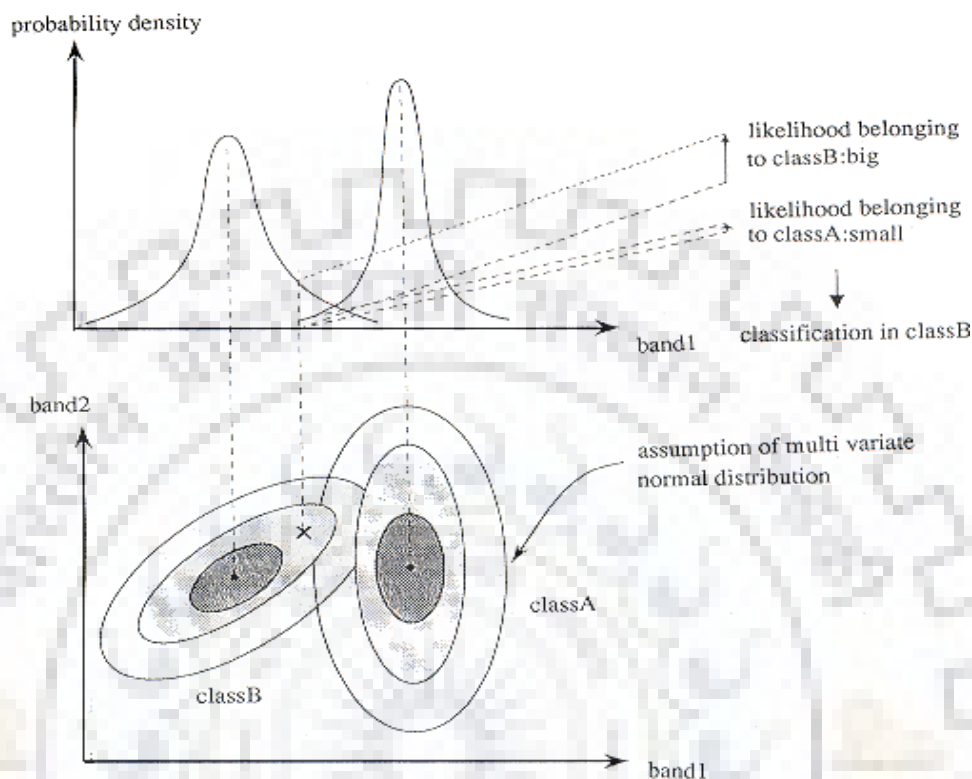

Figure 3.8 Concept of Maximum Likelihood method [2]

3.5 Ensemble Approach and ANN technique for Mixed Pixels

Mixed pixel is the summation of all energy reflected from the various bands of the multispectral image [7]. The reason for the mixed pixel is due to low spatial resolution that causes multiple classes to be present in same pixel which causes mixture of different endmembers. Spatial resolution is defined as individual pixel per inch. Better is the spatial resolution more clear is the image but it is not easily available and also cost-effective. Thus coarser resolution is taken into consideration. Now main challenge is the processing of coarser resolution into fine spatial resolution. It is difficult task to calculate the average area and boundaries due to mixed pixel. Various land cover classification [24] algorithms are applied to tackle this issue.

Un-mixing algorithms [25] were used calculating reflectance parameters. Endmembers are calculated for separation of pixels. Different probabilistic techniques like maximum likelihood [26] were computed for variance and covariance of each class which estimates the probability of a pixel of a class. But there is high correlation among variance and covariance matrices causing stability problems. Many supervised and unsupervised algorithms [27] have been used for appropriate classification of mixed pixels. Back-propagation technique and supervised learning algorithms such as maximum livelihood classifier techniques were correlated and the accuracy was compared. The problem caused by mixed pixel has been classified first using the supervised learning approach i.e. artificial neural network which is then

further compared with the ensemble learning approach using classifications such as Mahalanobis Distance classifier, Support Vector machines, Maximum Likelihood classifier

3.5.1 Artificial Neural Network

It is defined as correlation of layers of neurons, multilayer preceptor [28], [8]. It has three layers input layer, output layer and hidden layer. Layers include nodes that generate output on the basis of activation function. Weighted directed edges form the connection between the neurons, to modify it learning algorithms are used. The nodes are passive in input layers because they get the value and copied it to multiple layers while other nodes are hidden and outputs are active, they are used to modify the data. Accuracy can be improved by proper selection of weights.

The number of endmembers from the input data is calculated and training of samples is done in the input layer. Input layer tells about the spectral bands while the output layer tells about the endmembers. Backpropagation determined the difference between actual and expected outputs and error feedback to the network. It mainly determines the gradient of the objective function, which is further optimized and weights are updated to minimize the function. ANN flowchart is shown in Figure 3.9
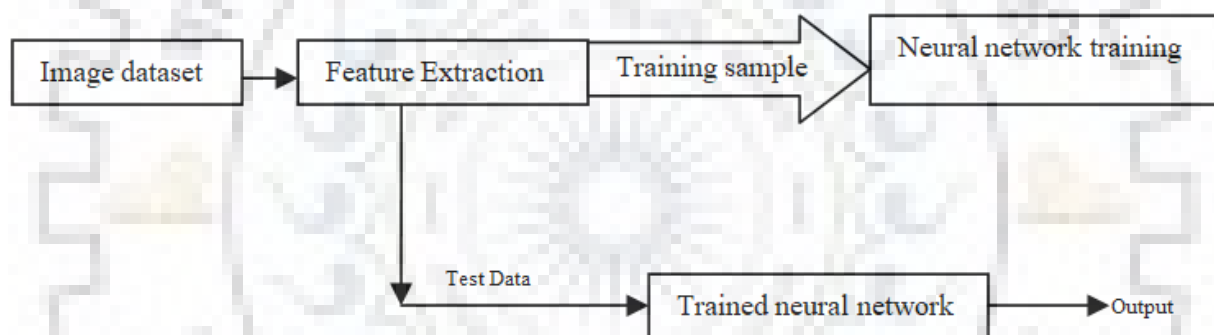
Figure 3.9 Flowchart for ANN [14]

3.5.2 Ensemble Learning

Ensemble is a procedure for taking mean of multiple classes for better implementation of the hypothesis. Several models can be mixed to form an optimum decision boundary [11] which is often a difficult process for a single classifier. The different types of ensemble learning algorithm for classification are:
- Use of different learning algorithm for classification and voting is done by combining the best result out of this used learning algorithm.
- Use of one algorithm with different choice of parameters for classification.
- Using of different data sets for training the model, like methods such as – Bagging, Boosting, Adaboost, and Stacking.
- Usage of same algorithm with same data sets having different features like Random subspace.

The ensemble learning is better as it takes best result out of all classifiers used. Ensemble draws perfect hypothesis with good approximation. In flowchart given below in Figure 3.10 for Ensemble learning it tells that voting is done in the decision tree from the output of 3 classifiers used. by combined voting we get the resultant Ensemble image.
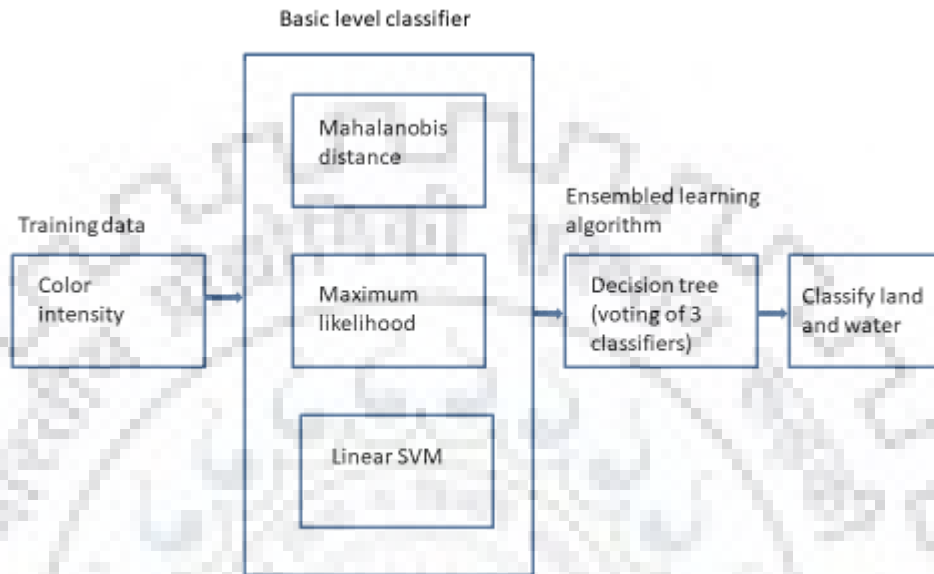

Figure 3.10 Flowchart for Ensemble approach

Backpropagation algorithm and Ensemble approach classifier has been applied to Sentinel-2 image for classification for time series data of the satellite images. Accuracy of both the methods have been compared for different dates of appearing of satellite images. Urban, Forest, and Water area in satellite image doesn't change much with time. Vegetation and soil area changes according to season as various crops harvest in different season and sometimes the barren land is there when no crop is grown. Thus vegetation and soil area for satellite images have been compared for different time periods.

3. 6 Soil And Urban Classification

Due to similar reflectance value of soil and urban classes it is challenging task to classify them on the basis of standard classification techniques using spectral features. Urban areas are mixture of different materials, e.g., concrete, asphalt, metal, plastic, and glass [14], [15], whose characteristics can be similar to other materials, such as bare land, fallow land, and sand [16], [17]. Various methodologies have been applied for urban and soil classification such as regression, ANN, spectral unmixing, object based classification methods, and built-up indices.

Due to simplicity and speed effectiveness various Radiometric and Built-up index based methods have resulted effectively to classify urban and soil [18], [19]. Soil and Urban classification from indices and textural feature is shown in Figure 3.11.

Sentinel -2 image is taken

↓

Making of image is done for classes other than urban and soil using NDVI values less than 0.2

↓

Various radiometric and built up index are calculated for the masked image on different spectral bands or textural features are computed for the image

↓

Separabilty index is measured for all the images

↓

Mean and standard deviation of classes is taken for image having good separability index

↓

Urban and soil classified image is made based on the threshold values of indices and textural features
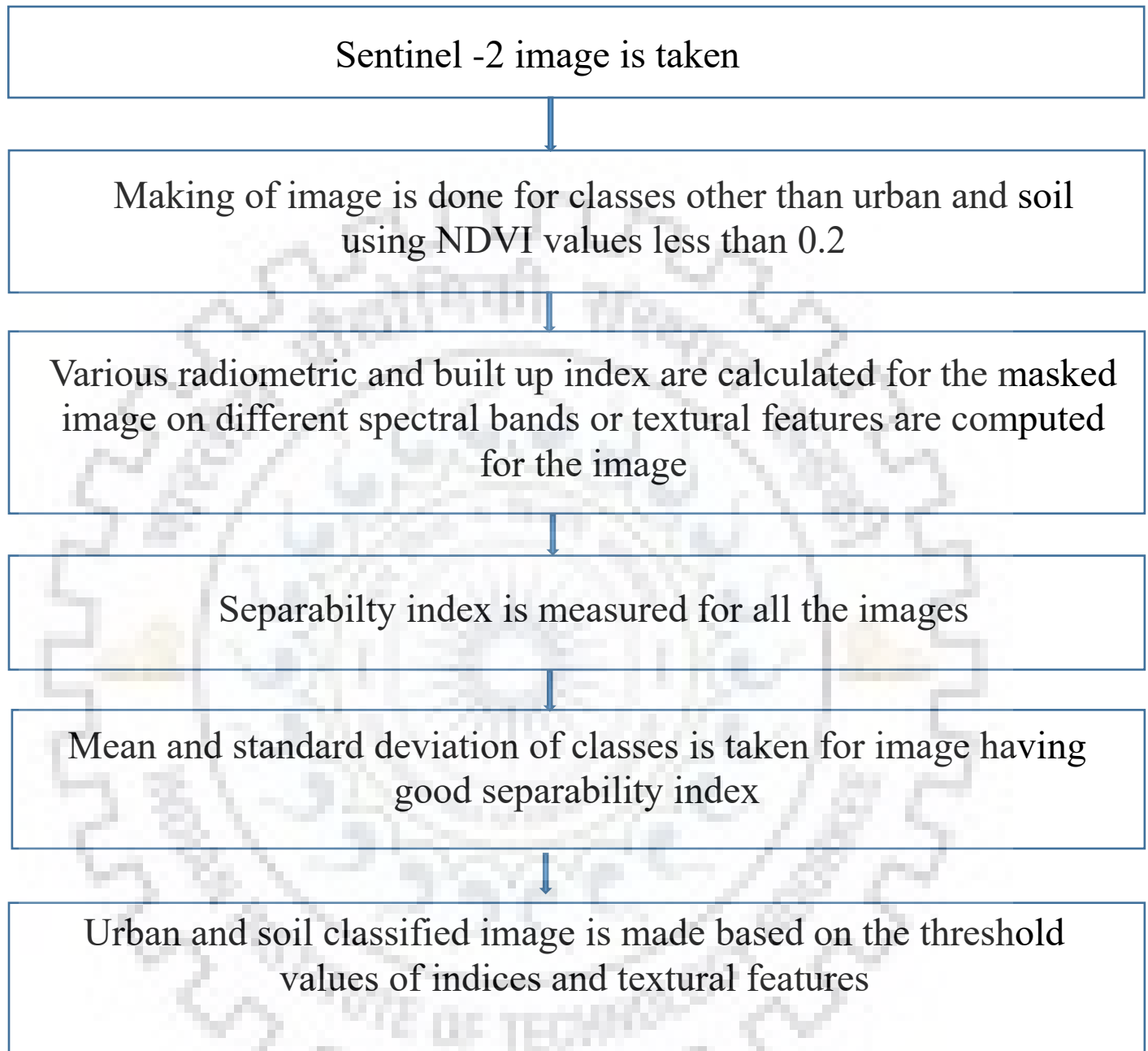
Figure 3. 11 Flowchart for Soil and Urban classification

3.6.1 Radiometric and Built-up Index methods

Built-up and Radiometric index based methods can be one of the good techniques for soil and urban extraction, because of their simplicity, easy implementation, and speed. These indices are used to distinguish between soil and built-up area by reducing the atmospheric and topographic effects if possible. Various types of indices like NBI, NBAI, BAEI, RI etc. are used for classification based on Separability Index values.

3.6.2 Textural Analysis

Improving the spatial resolution of the satellite images not always guarantee better outcome for classification using spectral techniques. Better spatial resolution reduces mixed pixels but increases subclasses which cause problem in classification of classes such as urban and soil. Spectral resolution tells about gray level variation of a pixel, whereas texture features gives information about the spatial distribution of the gray levels over an image. Some textural features are fractal dimension (D) [9], Second order co-occurrence parameters such as Mean, Entropy, Homogeneity, Second order moment, Variance, and Correlation. Our aim is to differentiate between the classes by using minimum features possible, the sensitivity analysis is carried out.

For demonstration of these features, region of interest for soil and urban classes are taken. The separability index is calculated for the images obtained from texture features. SI (Separability Index) of second order mean is suitable for proper classification between two classes.

Second-order (also called co-occurrence) metrics tells about the interrelation between pixel pairs. This matrix is a function of both the angular relationship and distance between two neighboring pixels. It gives the number of occurrences between a particular pixel and its neighbor. This is referred as a "gray-tone spatial-dependence matrix."

- Mean is essentially a smoothing function.
- Variance is an estimate of the values around the mean. This value is based on the Greyscale Quantization Level
- Homogeneity calculates by using the "inverse difference moment" equation. Values range from 0 to 1.0.
- Entropy is used for computing the randomness in an image. It also measures the uncertainty in the area of interest.
- Second moment value varies from 1 to 10. It is also based on second order co-occurrence matrices.
- Correlation is used for the measurement of the linear dependencies present in an image pertaining to the gray tone.

3.7 Estimation of Fractional Vegetation Cover Using Spectral Mixture Analysis

Fractional vegetation cover (FVC) is defined as vertical area covered by vegetation to the total ground area projected. FVC is quite essential for many environmental implementations, such as vegetation

models [30], soil erosion models [31], and weather prediction models [11]. For calculating FVC, Remote sensing techniques are good alternative and being less expensive methods due to good spatial and temporal resolution. Several algorithms have been proposed on remotely sensed data, including different regression models related to vegetation index, and spectral mixture analysis (SMA) [12], [13]. Normally, land areas consist of different land covers. SMA breaks the mixed pixels that are present in a pixel into fractional components i.e. different endmembers present.

Spectral Mixture Analysis is a method that determines the organization of each pixel present in the image. Mixed pixels are the pixels which contain more than one class within single pixel. "Pure" pixels contain only one class or feature. For example, a pure pixel would contain only one feature such as urban cover and a mixed pixel might contain vegetation, built-up class, and soil crust. In different traditional classification algorithm mixed pixel will create problem as they classify pixel into only one class.

SMA determines the parts of mixed pixels by estimating a particular class based on the spectral characteristics of its endmembers. Spectral endmembers are the 'pure' spectra of each land cover class. The definition of land cover classes and selection of correct endmembers for each class are both important in SMA. Endmembers from the actual image are mostly preferred because no calibration is needed between selected endmembers and the measured spectra. Endmembers are the purest pixels present in the image.
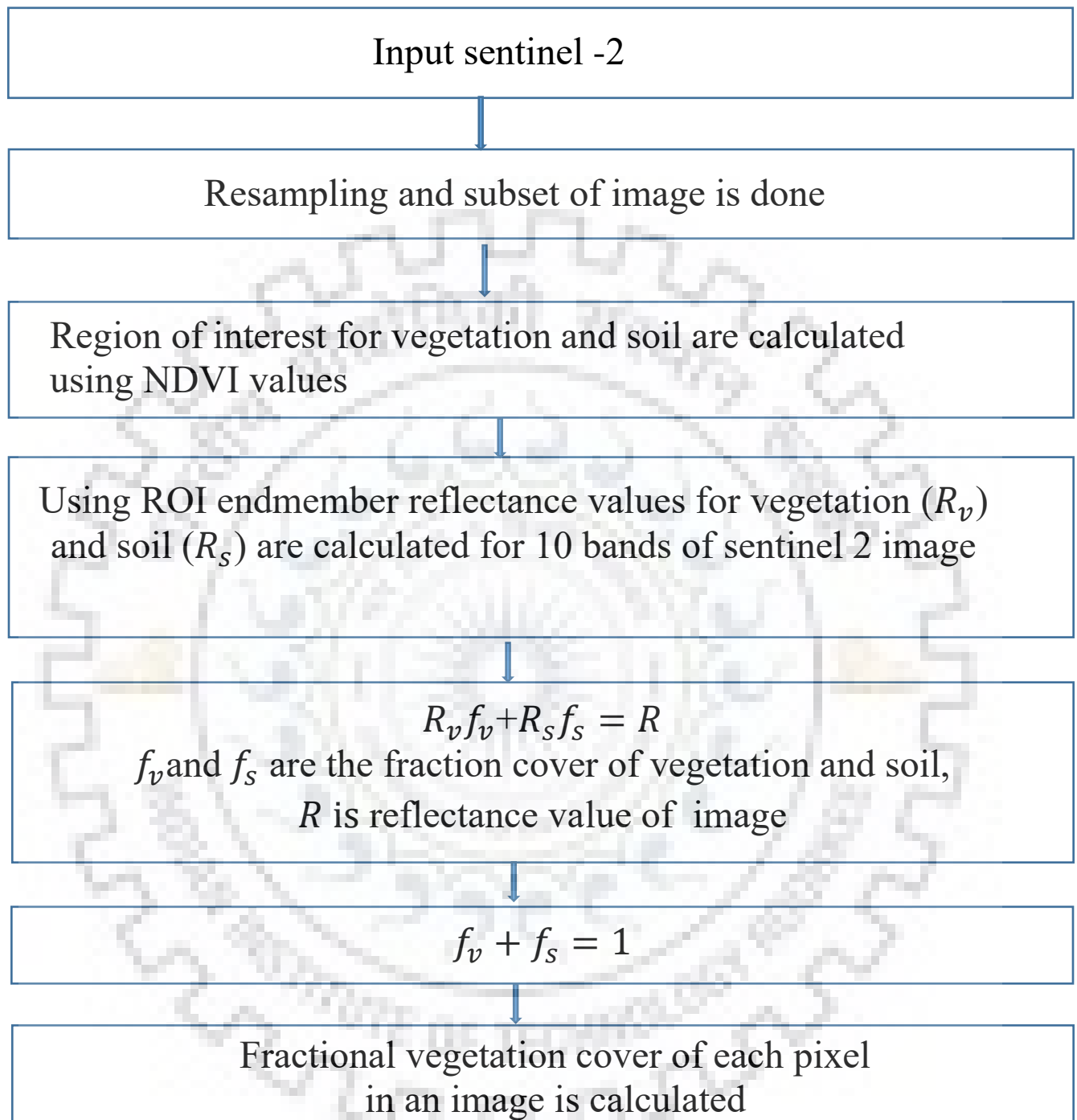
Input sentinel -2

Resampling and subset of image is done

Region of interest for vegetation and soil are calculated using NDVI values

Using ROI endmember reflectance values for vegetation (R_v) and soil (R_s) are calculated for 10 bands of sentinel 2 image

$$R_v f_v + R_s f_s = R$$
f_v and f_s are the fraction cover of vegetation and soil, R is reflectance value of image

$$f_v + f_s = 1$$

Fractional vegetation cover of each pixel in an image is calculated

Figure 3. 12 Flowchart for calculating FVC

CHAPTER 4

RESULTS AND DISCUSSION

4.1 Classification results for Masking technique

Flowchart for masking technique has been briefly explained in section 3.3. The results of masking have been described below.

Figure 4.1 Water mask (Data Id No. 7)

Water masking has been done by considering Red and Near Infrared (NIR) bands. Reflectance values for both bands have been calculated by taking region of interest. Range of reflectance value for NIR band is in between 0.0518 to 0.0979 and for Red band is in between 0.0789 and 0.1146.
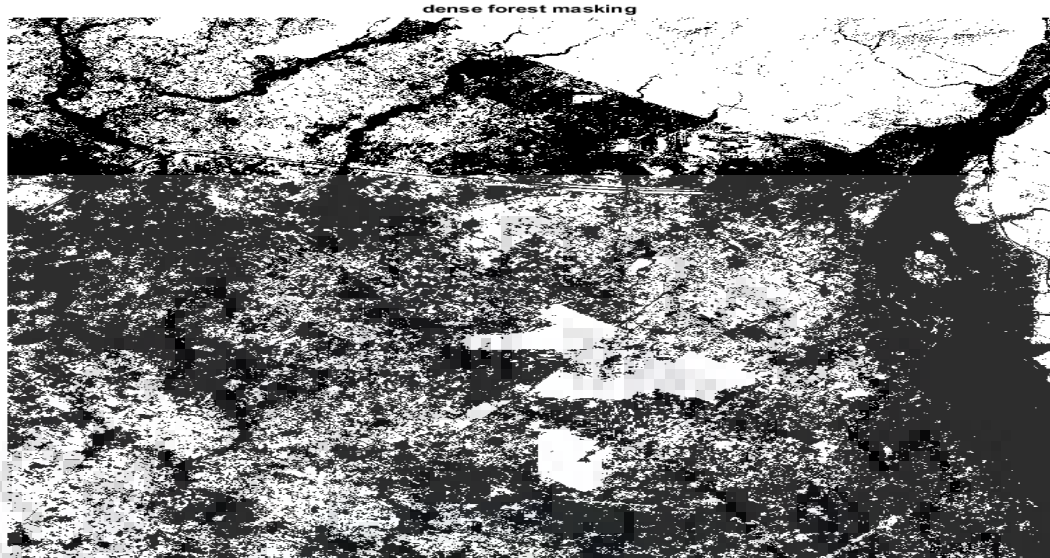
Figure 4.2 Forest mask (Data Id No. 7)

Forest mask is created by considering Green and NIR band. Range of reflectance value for NIR band is in between 0.063 and 0.2612 and for Green band range is 0.076 and 0.1168 which have been calculated by taking region of interest.
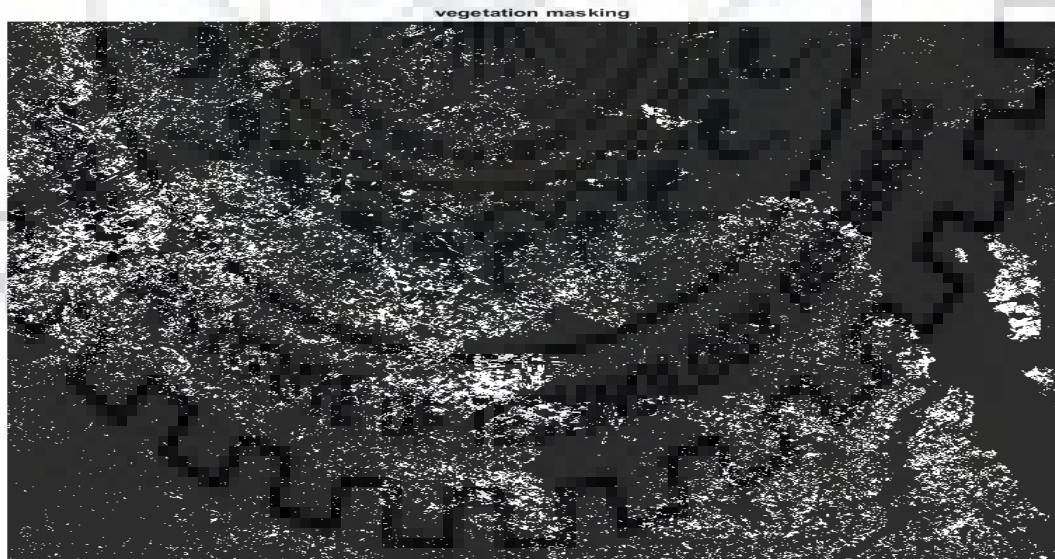

Figure 4.3 Vegetation mask (Data Id No. 7)

Vegetation mask is created by considering Green and NIR band. Range of reflectance value for NIR band is in between 0.2114 and 0.3268 and for Green band range is 0.1169 and 0.138.
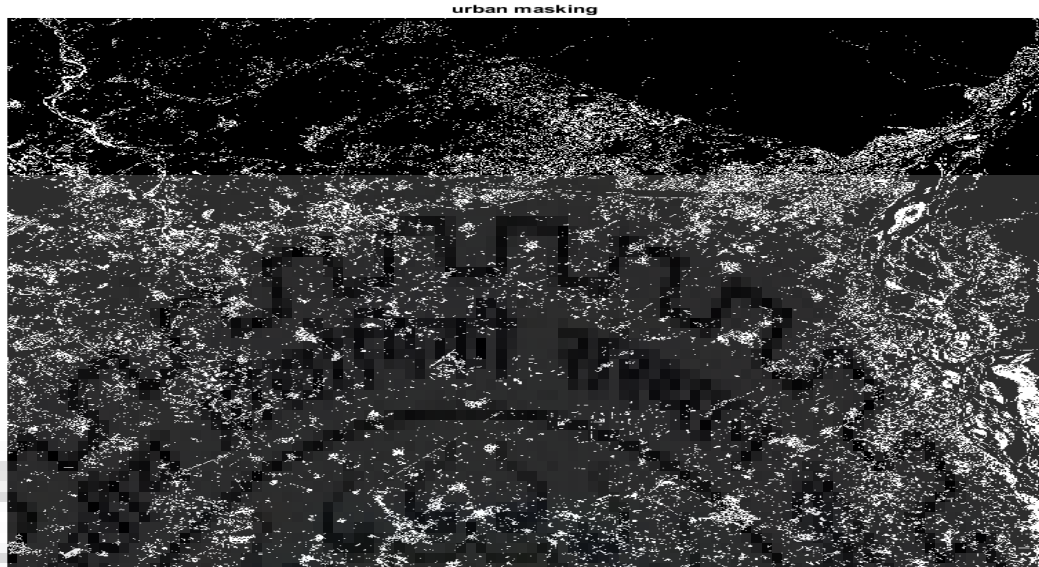
Figure 4.4 Urban mask (Data Id No. 7)

Urban mask is created by considering Green and Red band. Range of reflectance value for Red band is in between 0.112 and 0.136 and for Green band range is 0.1268 and 0.147.

Figure 4.5 Barren mask (Data Id No. 7)

Barren mask is created by considering Blue and Red band. Range of reflectance value for Red band is in between 0.1361 and 0.2115 and for Blue band range is 0.1471 and 0.2086.
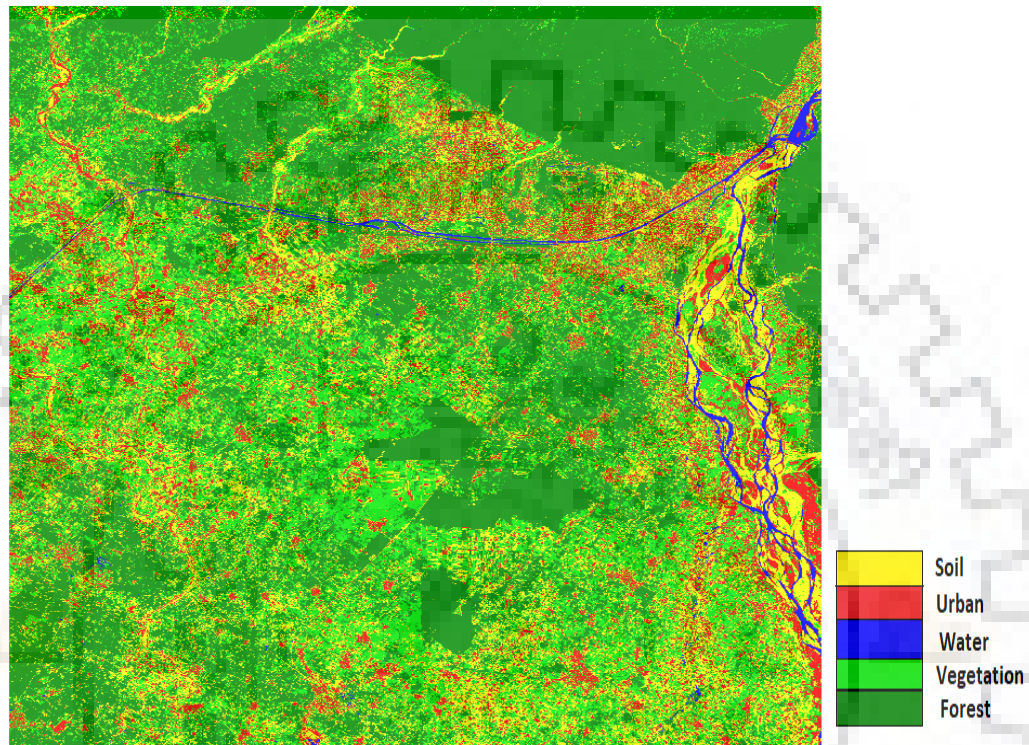

Figure 4.6 Sentinel-2 Image with Masks Applied (Data Id No. 7)

Masking technique has been applied on the Sentinel-2 image and area has been calculated by pixel counting for different classes taken. The size of the image is 3000*3000 pixels and area of each pixel is 10*10 square meter. Thus total image area comes out to be 900 square kilometer. By using masking area of various classes is as follows:

- Area of class Water= 9.93 square kilometer
- Area of class Urban= 100.60 square kilometer
- Area of class Barren land= 164.02 square kilometer
- Area of class Vegetation= 253.19 square kilometer
- Area of class Forest= 372.23 square kilometer

4.2 Classification result of Unsupervised techniques

Unsupervised classification techniques are briefly explained in section 3.4 whose results are shown in this section for accuracy analysis.

4.2.1 ISOdata

In section 3.4.1.1 ISOdata classification technique has been explained briefly. It tells about how the splitting and merging of clusters occurs in the classification technique. Overall efficiency of ISOdata algorithm is coming out to be 71.15%.
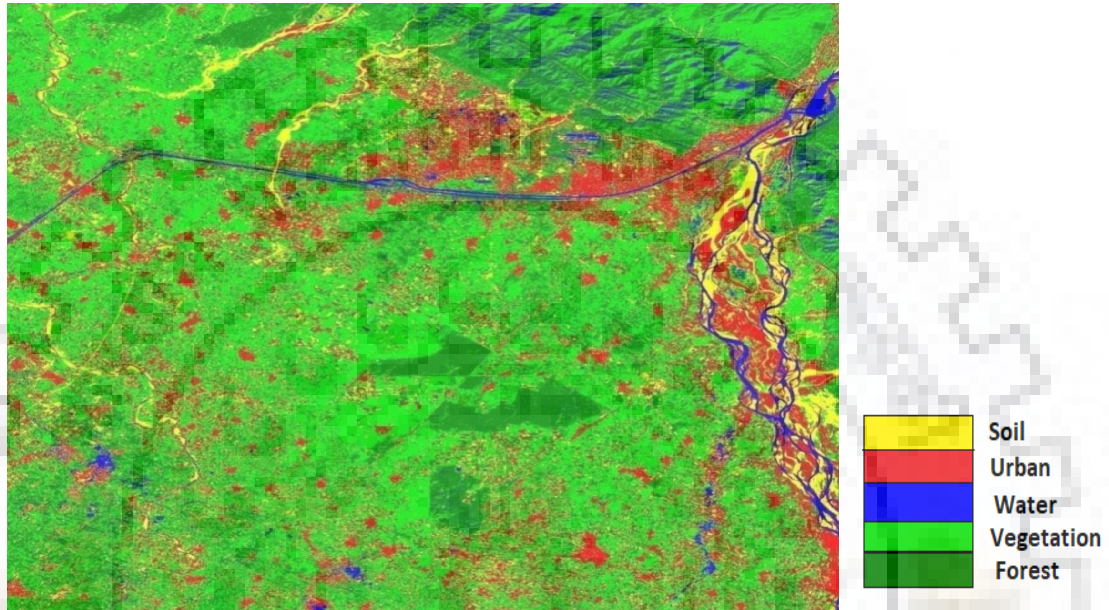

Figure 4.7 Sentinel-2 image after ISOdata classification (Data Id No. 7)

Table 4.1 Confusion matrix for ISOdata classifier

Class	Water	Vegetation	Urban	Barren	Forest	Total	User accuracy(%)
Water	209	46	1	0	9	265	78.87
Vegetation	0	229	26	22	61	338	67.75
Urban	1	96	153	13	0	263	58.17
Barren	0	60	22	240	0	322	74.53
Forest	0	36	3	7	163	209	77.99
Total	210	467	205	282	233	1397	
Producer accuracy(%)	99.52	49.04	74.63	85.11	69.96		71.15

4.2.2 K-Means

K-Means algorithm for unsupervised classification has been explained briefly in section 3.4.1.2. Total accuracy of K-means unsupervised algorithm is coming out to be 78.45% which is been calculated with the confusion matrix.
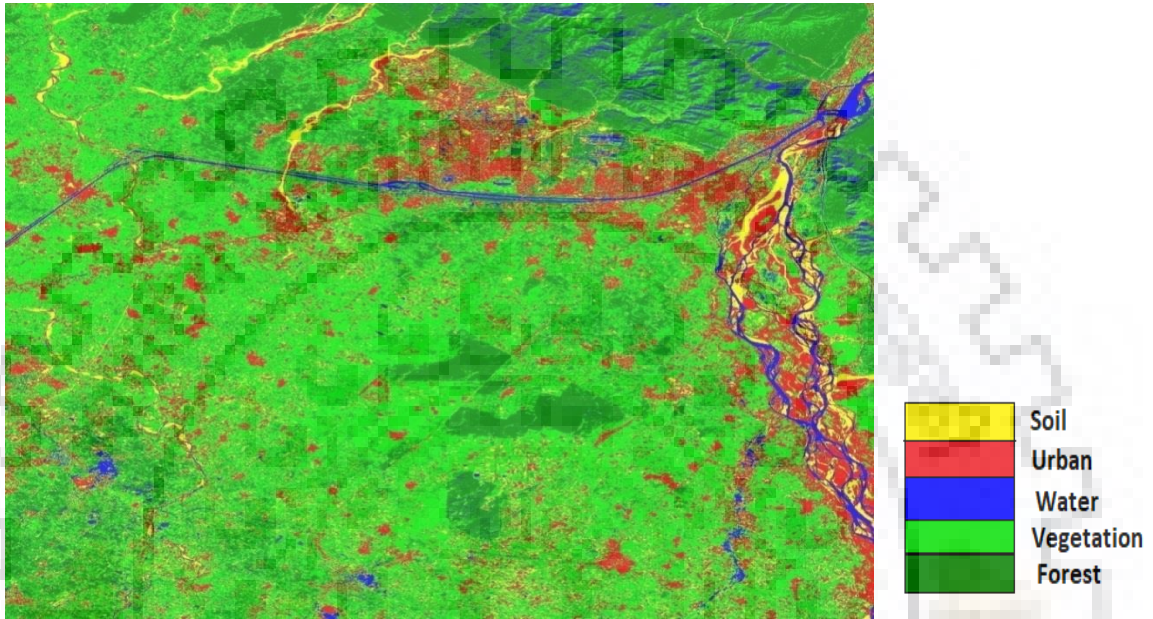

Figure 4.8 Sentinel-2 image after K-means classification (Data Id No. 7)

Table 4.2 Confusion matrix for K-means classifier

Class	Water	Vegetation	Urban	Barren	Forest	Total	User accuracy(%)
Water	209	45	0	1	0	265	78.87
Vegetation	1	305	34	45	4	389	78.41
Urban	0	31	35	149	0	215	69.30
Barren	0	56	213	10	0	279	76.34
Forest	0	29	0	0	220	249	88.35
Total	210	467	282	205	233	1397	
Producer accuracy(%)	99.52	65.31	75.53	72.68	94.42		78.45

4.3 Classification results of Supervised techniques

Supervised classification techniques such as Parallelepiped Classifier, Minimum Distance, Mahalanobis Distance, Support Vector Machine and Maximum Likelihood Classifier have been explained in section 3.4.

4.3.1 Parallelepiped Classifier

The parallelepiped classification technique for Supervised classification is explained in section 3.4.2.1.Overall efficiency of supervised Parallelepiped classifier is 65.56%. Its result is misclassified because of particular pixel value not lying in the boxes range of specific class.
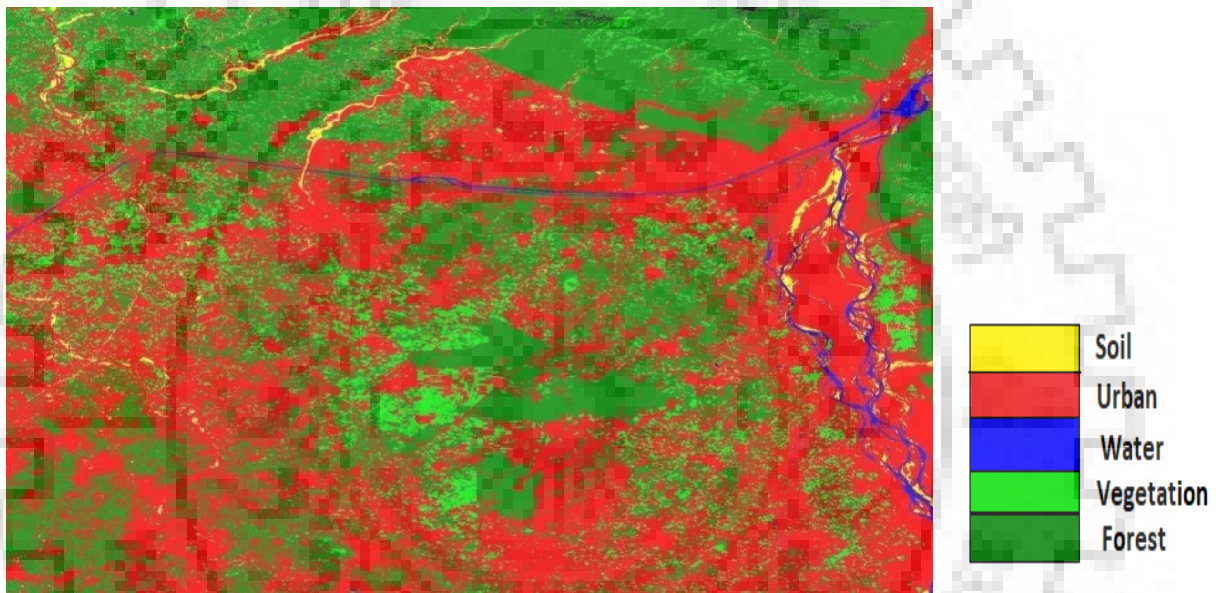

Figure 4.9 Sentinel-2 image after parallelepiped classifier (Data Id No. 7)

Table 4.3 Confusion matrix for Parallelepiped classifier

Class	Forest	Water	Urban	Vegetation	Barren	Total	User accuracy(%)
Forest	232	0	0	40	0	272	85.29
Water	0	206	0	16	0	222	92.79
Urban	0	3	203	296	122	624	32.53
Vegetation	1	1	0	115	0	117	98.29
Barren	0	0	1	0	160	161	99.38
Total	233	210	205	467	282	1397	
Producer accuracy(%)	99.57	98.10	99.02	24.63	56.74		65.56

4.3.2 Mahalanobis Distance classifier

Mahalanobis Distance classifier is explained in section 3.4.2.2. It tells about how Euclidean distance is calculated by removing the covariance between elements. Overall efficiency of Mahalanobis distance is 74.01%
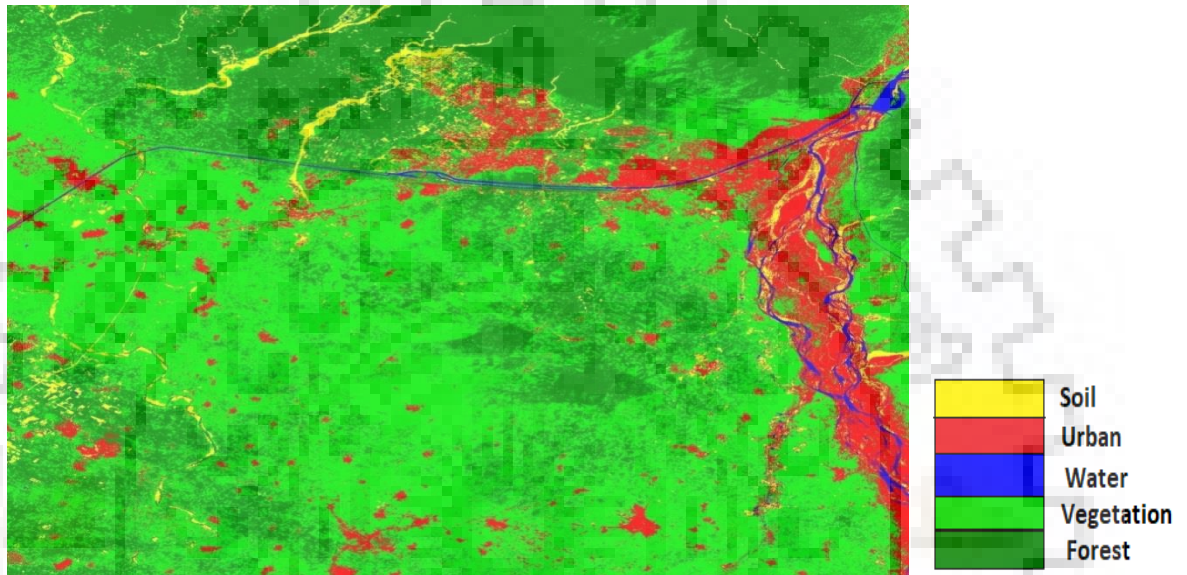

Figure 4.10 Sentinel-2 image after Mahalanobis Distance classifier (Data Id No. 7)

Table 4.4 Confusion matrix for Mahalanobis Distance classifier

Class	Forest	Water	Urban	Vegetation	Barren	Total	User accuracy(%)
Forest	207	0	4	60	4	275	75
Water	0	195	0	20	0	215	90.70
Urban	0	14	178	154	48	394	45.18
Vegetation	26	1	10	233	9	279	83.51
Barren	0	0	13	0	221	234	94.44
Total	233	210	205	467	282	1397	
Producer accuracy(%)	88.94	92.86	86.83	49.29	78.37		74.01

4.3.3 Minimum Distance classifier

Minimum Distance classifier is explained briefly in the section 3.4.2.3. Overall efficiency of Minimum Distance classifier is 83.24%.
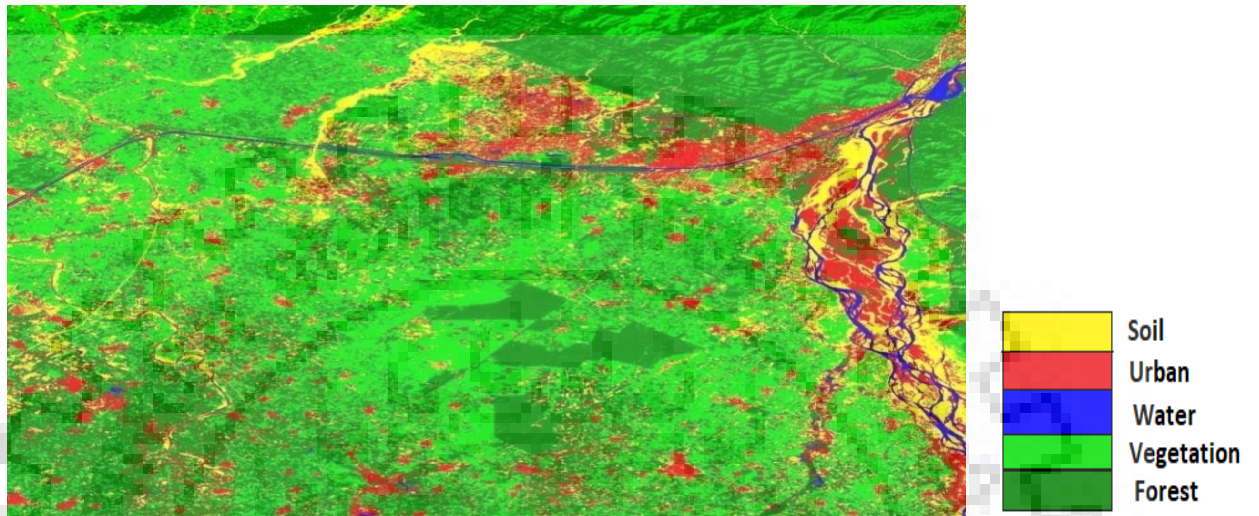

Figure 4.11 Sentinel-2 image after Minimum Distance classifier (Data Id No. 7)

Table 4.5 Confusion matrix for Minimum Distance classifier

Class	Forest	Water	Urban	Vegetation	Barren	Total	User accuracy(%)
Forest	213	0	0	65	0	278	76.62
Water	2	209	0	21	0	232	90.09
Urban	0	1	190	68	42	301	63.12
Vegetation	18	0	2	311	0	331	93.96
Barren	0	0	13	2	240	255	94.2
Total	233	210	205	467	282	1397	
Producer accuracy(%)	91.42	99.52	92.68	66.60	85.11		83.24

4.3.4 Support Vector Machine

Support vector machine uses hyperplanes and different type of kernels which has been explained in section 3.4.2.4. Overall efficiency of SVM classifier is coming out to be 91.91%.
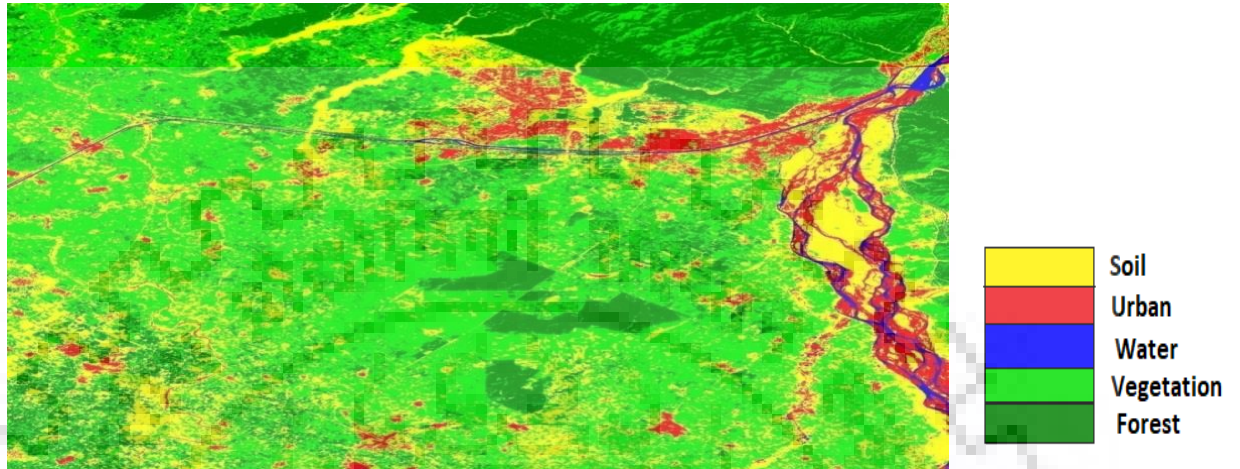

Figure 4.12 Sentinel-2 image after SVM classifier (Data Id No. 7)

Table 4.6 Confusion matrix for SVM classifier

Class	Forest	Water	Urban	Vegetation	Barren	Total	User accuracy(%)
Forest	227	0	0	2	0	229	99.13
Water	0	207	0	9	0	216	95.83
Urban	0	1	165	27	16	209	78.95
Vegetation	6	2	22	428	9	467	91.65
Barren	0	0	18	1	257	276	93.12
Total	233	210	205	467	282	1397	
Producer accuracy(%)	97.42	98.57	80.49	91.65	91.13		91.91

4.3.5 Maximum Likelihood Classifier

Maximum Likelihood classifier uses probability density function for classification of pixels which is explained in detail in section 3.4.2.5. Overall efficiency of Maximum Likelihood Estimation is 92.84%.
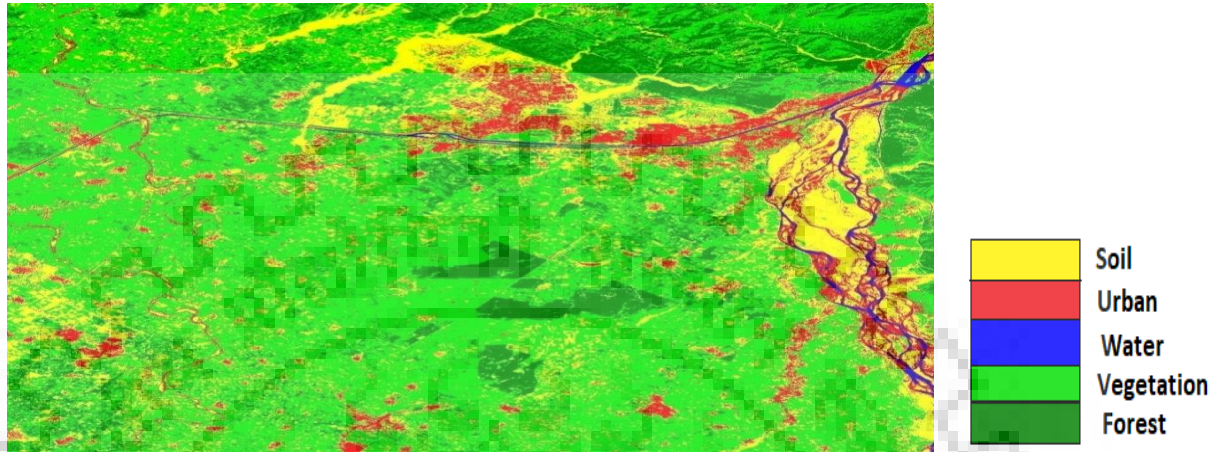

Figure 4.13 Sentinel-2 image after MLE classifier (Data Id No. 7)

Table 4.7 Confusion matrix for MLE classifier

Class	Forest	Water	Urban	Vegetation	Barren	Total	User accuracy(%)
Forest	231	0	0	3	0	234	98.72
Water	0	205	0	0	0	205	100
Urban	0	1	190	59	15	265	71.70
Vegetation	2	4	3	405	1	415	97.59
Barren	0	0	12	0	266	278	95.68
Total	233	210	205	467	282	1397	
Producer accuracy(%)	99.14	97.62	92.68	86.72	94.33		92.84

By using Supervised Machine learning technique of Maximum Likelihood Estimation technique which gives the best result having overall accuracy of 92.84%. Area of various classes is as follows:

- Area of class Water= 7.53 square kilometer
- Area of class Urban= 72.93 square kilometer
- Area of class Forest= 126.52 square kilometer
- Area of class Barren land= 185.77 square kilometer
- Area of class Vegetation= 507.2 square kilometer

4.4 Ensemble approach vs Backpropagation algorithm

Ensemble approach for mixed pixel and Backpropagation algorithm application on Sentinel-2 image has been explained briefly in section 3.5. Results of both the algorithm are compared in this section. In Ensemble approach voting is done by using three classifiers namely Mahalanobis Distance, Support vector machine and Maximum likelihood classifier.

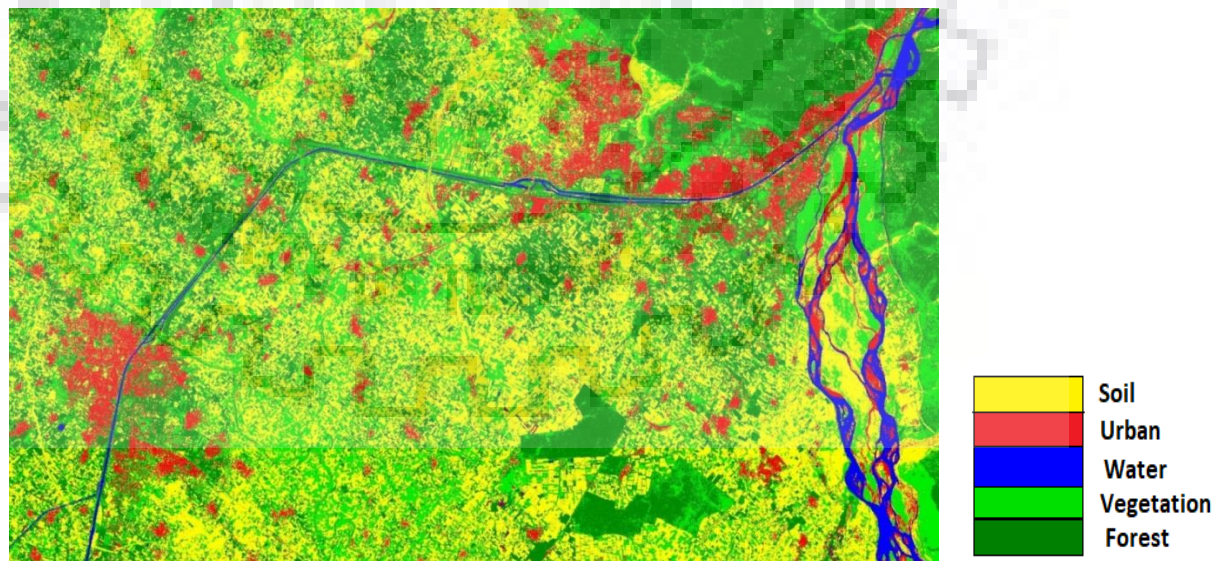**Figure 4.14 Sentinel- 2 RGB (Red- Band 4, Green- Band 3, Blue- Band 1) image (25 April 2019)**

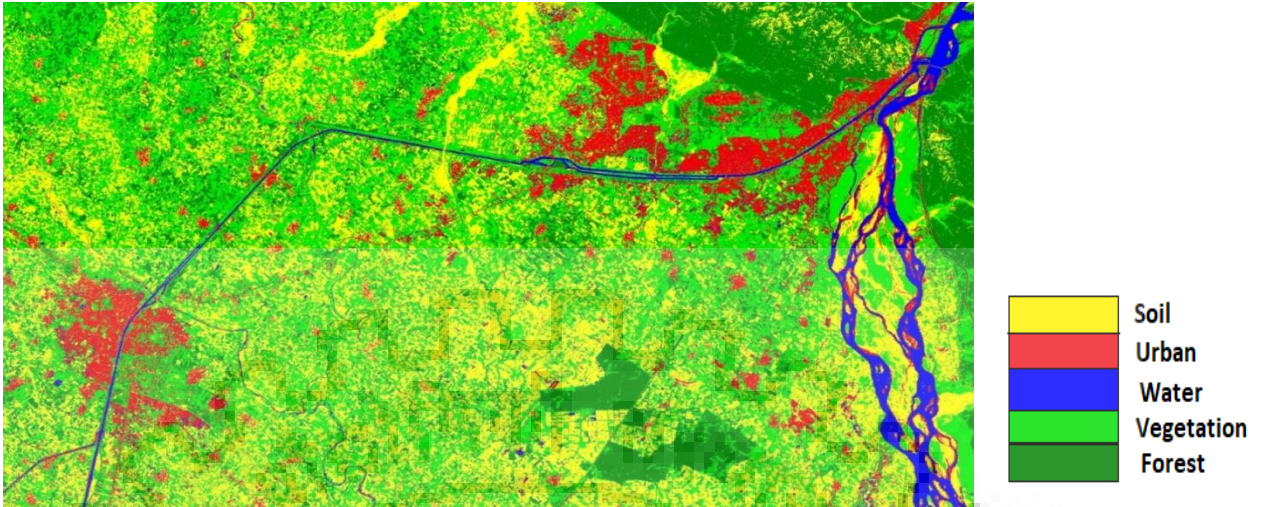**Figure 4.15 Mahalanobis Distance Classifier (Data Id No. 1)**

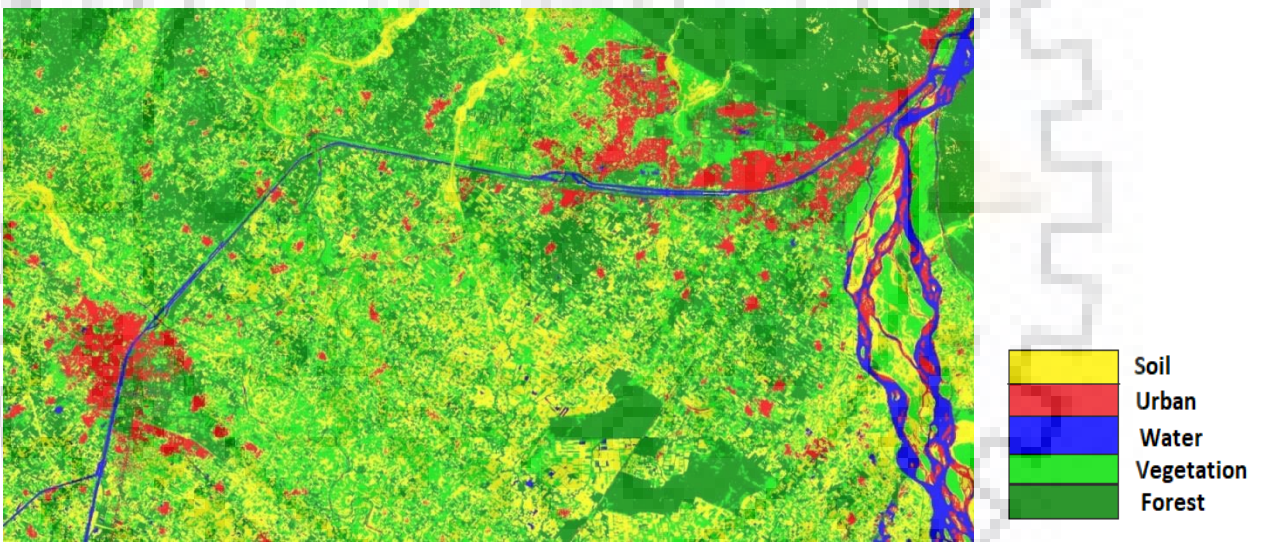**Figure 4.16 Maximum likelihood classifier (Data Id No. 1)**

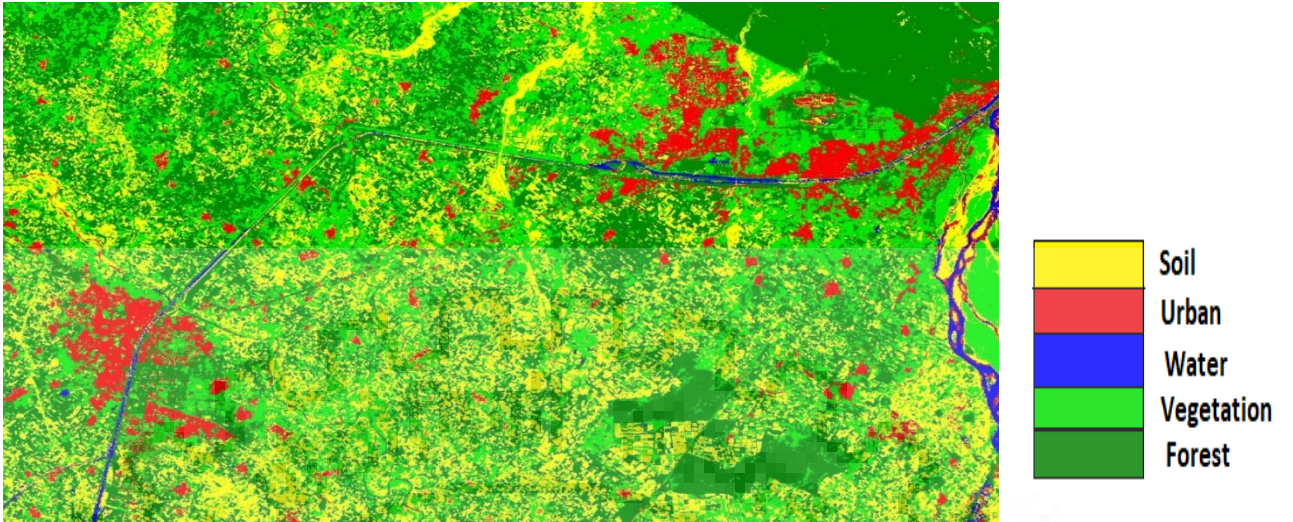**Figure 4.17 Support vector machine classifier (Data Id No. 1)**

Figure 4.18 Backpropagation Algorithm for classification (Data Id No. 1)
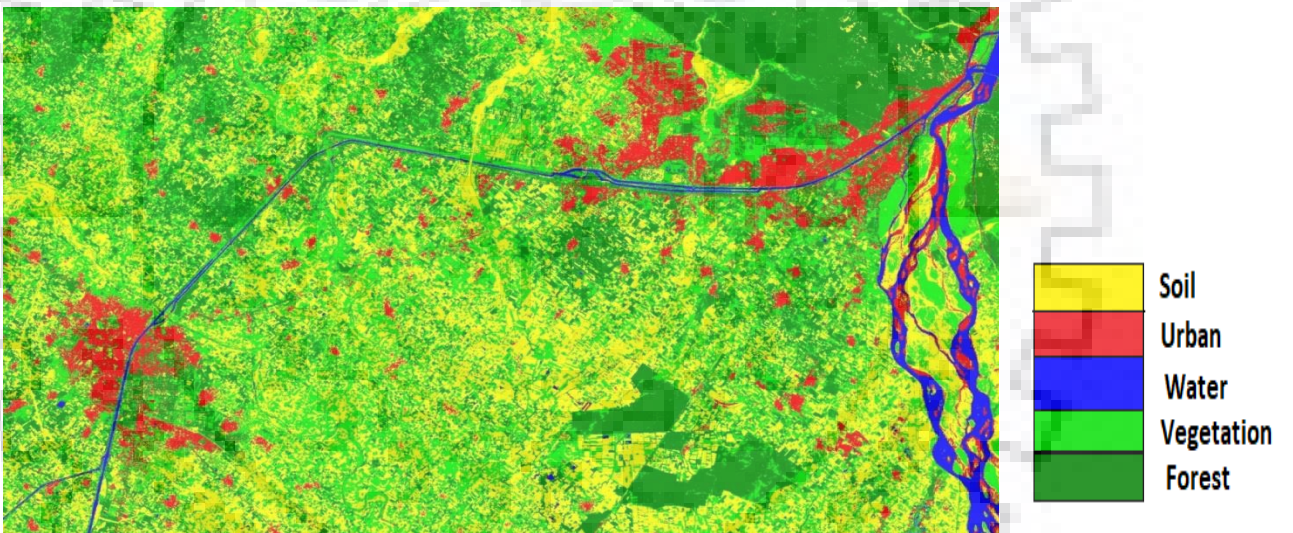

Figure 4.19 Ensemble approach (Data Id No. 1)

Similarly, Sentinel-2 image has been taken for 6 other days for different parts of the year and results have been compared for Ensemble and Backpropagation Algorithm.

Table 4.8 Accuracy Assessment

Sentinel-2 image	Ensemble Approach (OA)	Backpropagation Algorithm (OA)	Vegetation Area (Sq. Km)	Soil Area (Sq. Km)
25 April 2019	94.67%	92.94%	186.3	213.4
15 April 2019	92.85%	93.29%	172.6	144.9
14 February 2018	96.31%	95.37%	305.61	87.75
22 October 2017	97.20%	97.06%	360.84	85.82
7 October 2017	98.16%	97.63%	269.5	69.8
10 April 2017	93.50%	94.10%	170.5	119.12
11 December 2016	97.52%	98.45%	221.26	139.73

OA- Overall classification Accuracy

Accuracy assessment of Ensemble learning and Backpropagation algorithm have been described in above tables. The testing of results has been performed for satellite images in different days throughout the year. Ensemble learning approach has shown better accuracy as compared to the other.

4.5 Soil and Urban classification

Soil and urban can be classified based on two methods namely Radiometric and Built-up indices and Textural features which has been explained briefly in section 3.6.

4.5.1 Radiometric and Built-up indices

4.5.1.1 NBI

The new built-up index (NBI) was calculated using RED, NIR, and SWIR bands [33].
NBI is defined as follows:

$$NBI = \frac{B_R B_{SWIR}}{B_{NIR}}$$

(22)

Red (B_R) is band 4, SWIR (B_{SWIR}) is band 11 and NIR (B_{NIR}) is band 5 of Sentinel-2 image.
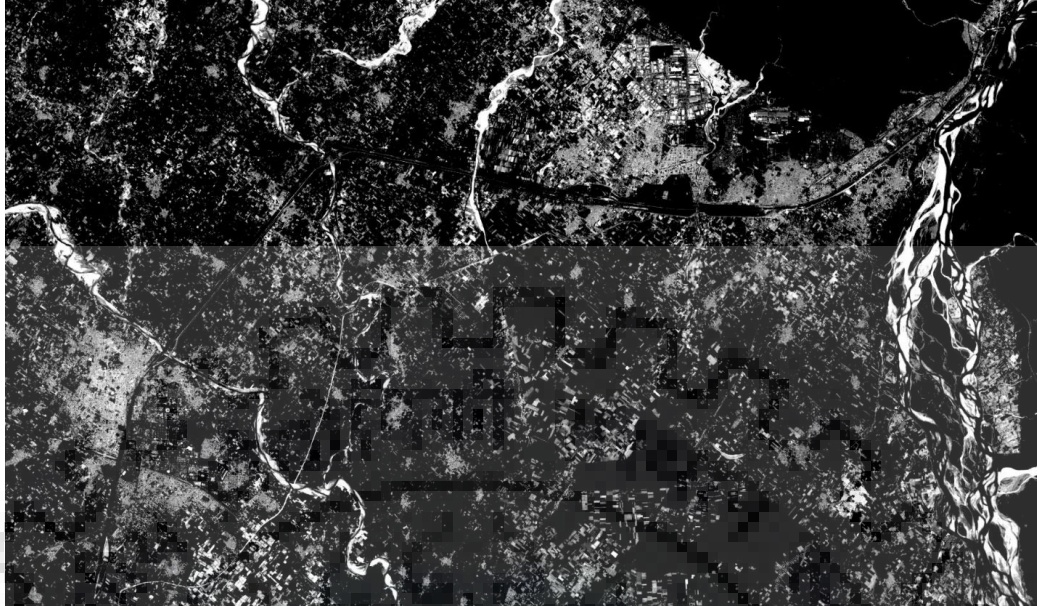
Figure 4. 20 NBI masked image

4.5.1.2 NDTI

Normalized Difference Tillage Index is an index that separates urban from different locations present in the image. NDTI [28] results show that it is higher for pixels having bare land than as compared to pixels of urban areas thus differentiating two areas.

$$NDTI = \frac{B_{SWIR1} - B_{SWIR2}}{B_{SWIR1} + B_{SWIR2}}$$ (23)

SWIR 1 (B_{SWIR1}) is band 11 and SWIR 2 (B_{SWIR2}) is band 12 of Sentinel-2 image.

Figure 4.21 NDTI masked image (Data Id No. 4)

4.5.1.3 NBAI

Waqar et al. introduced indices named normalized built-up area index (NBAI) [33].
Where B_{SWIR2} is another SWIR band, satisfying that $B_{SWIR2}<B_{SWIR1}$.

$$NBAI = \frac{B_{SWIR1} - B_{SWIR2}/B_{green}}{B_{SWIR1} + B_{SWIR2}/B_{green}} \tag{24}$$

SWIR 1 (B_{SWIR1}) is band 11, SWIR 2 (B_{SWIR2}) is band 12 and Green (B_{green}) is band 3 of Sentinel-2 image.

Figure 4.22 NBAI masked image (Data Id No. 4)

4.5.1.4 BAEI

The built-up area extraction index uses Red, Green, and SWIR bands. It uses an arithmetic constant L=0.3 to compute the index:

$$BAEI = \frac{B_R + 0.3}{B_{SWIR} + B_G} \tag{25}$$

Red (B_R) is band 4, SWIR (B_{SWIR}) is band 11, and Green (B_G) is band 3 of Sentinel-2 image.

Figure 4.23 BAEI masked image (Data Id No. 4)

4.5.1.5 NDBI

The normalized difference built-up index (NDBI) [9] uses NIR and SWIR bands according to the expression:

$$NDBI = \frac{B_{SWIR} - B_{NIR}}{B_{SWIR} + B_{NIR}} \qquad (26)$$

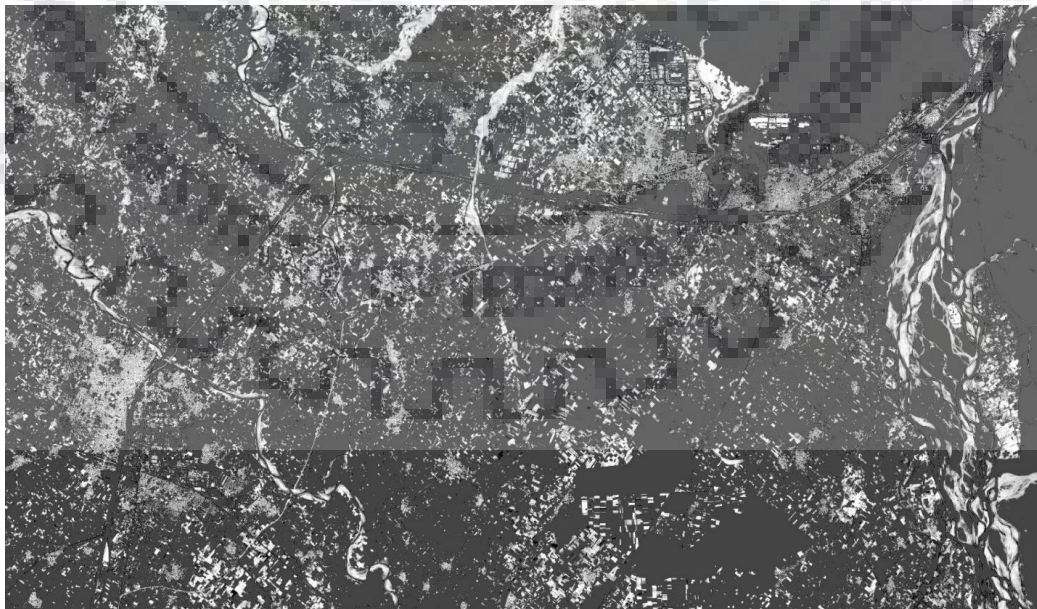SWIR (B_{SWIR}) is band 11, NIR (B_{NIR}) is band 5 of Seninel-2 image.

Figure 4.24 NDBI masked image (Data Id No. 4)

4.5.1.6 BI

The Brightness Index algorithm is representing the average of the brightness of a satellite image. The result looks like a panchromatic image with the same resolution of the original image. This index is therefore sensitive to the brightness of soils relating to humidity and the presence of salts in surface:

$$BI = \sqrt{\frac{B_R^2 + B_G^2}{2}} \tag{27}$$

Red (B_R) is band 4 and Green (B_G) is band 3 of Sentinel-2 images.

Figure 4.25 BI masked image (Data Id No. 4)

4.5.1.7 RI

The Redness Index algorithm was developed to identify soil color variations. The RI results from the following equation:

$$RI = \frac{B_R^2}{B_G^3} \tag{28}$$

Red (B_R) is band 4 and Green (B_G) is band 3 of Sentinel-2 images.

Figure 4.26 RI masked image (Data Id No. 4)

4.5.1.8 CI

The colour Index algorithm was developed to differentiate soils in the field. Low valued CIs have been shown to be correlated with the presence of a high concentration of carbonates or sulfates and higher values to be correlated with crusted soils and sands in arid regions.

In most cases the CI gives complementary information with the BI and the NDVI. Used for diachronic analyses, they help for a better understanding of the evolution of soil surfaces. The CI results from the following equation:

$$CI = \frac{B_R - B_G}{B_R + B_G} \qquad (29)$$

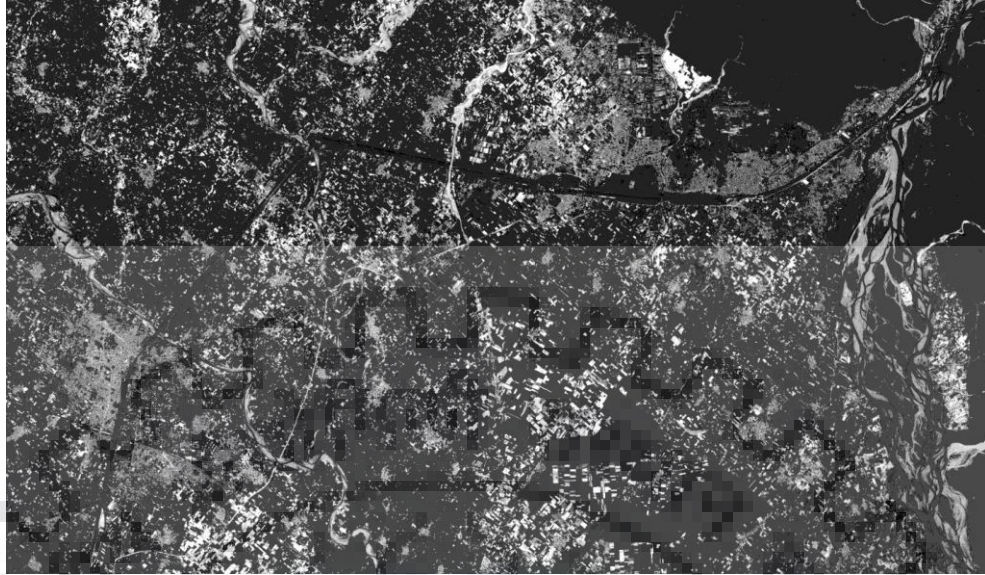Red (B_R) is band 4 and Green (B_G) is band 3 of Sentinel-2 images.

Figure 4.27 CI masked image (Data Id No. 4)

Table 4.9 Separability index calculation for various indices

Indices	Formulae	Separability Index
NBI	$\dfrac{B_R\,B_{SWIR}}{B_{NIR}}$	0.824
NDTI	$\dfrac{B_{SWIR1} - B_{SWIR2}}{B_{SWIR1} + B_{SWIR2}}$	0.08
NBAI	$\dfrac{B_{SWIR1} - B_{SWIR2}/B_{green}}{B_{SWIR1} + B_{SWIR2}/B_{green}}$	0.4
BAEI	$\dfrac{B_R + 0.3}{B_{SWIR} + B_G}$	1.46
NDBI	$\dfrac{B_{SWIR} - B_{NIR}}{B_{SWIR} + B_{NIR}}$	0.73
BI	$BI = \sqrt{\dfrac{B_R^2 + B_G^2}{2}}$	0.51
RI	$\dfrac{B_R^2}{B_G^3}$	0.27
CI	$\dfrac{B_R - B_G}{B_R + B_G}$	0.70

According to results shown BAEI shows good result to classify soil and urban based on Separability Index calculation as shown in Table 4.10. So classification result of BAEI classified image is taken as shown in Figure 4.28. Soil and Urban classes have been classified having threshold value of 1.19 i.e. it is soil when value of index is less than 1.19 and class is urban when index value is above 1.19.
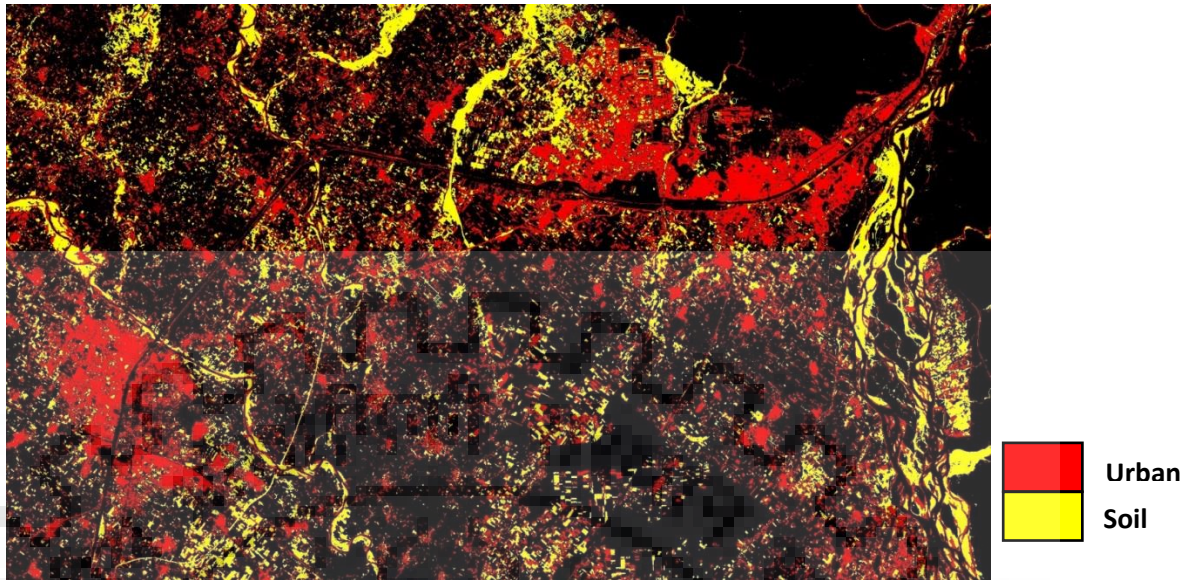
Figure 4.28 BAEI classified image (Data Id No. 4)

Accuracy Assessment

Overall Accuracy= 93.85%
Kappa Coefficient= 0.86

Table 4.10 Accuracy calculation for BAEI

Class	Built-up Area (pixels)	Soil Area (pixels)	Total no. of pixels	Sensitivity	Specificity
Built-up Area	323	53	376	0.982	0.916
Soil Area	6	578	584	0.916	0.982

4.5.2 Textural Analysis

Table 4.11 Separability index for textural features

Second order textural features	Formula	Separability Index
Mean	$$Mean = \sum_{i=1}^{N_g}\sum_{j=1}^{N_g} i * P(i,j)$$	1.51
Homogeneity	$$Homogeneity = \sum_{i=1}^{N_g}\sum_{j=1}^{N_g} \frac{1}{1+(i-j)^2}P(i,j)$$	0.11
Entropy	$$Entropy = \sum_{i=1}^{N_g}\sum_{j=1}^{N_g} P(i,j)\log P(i,j)$$	0.206
Second Moment	$$Second\ moment = \sum_{i=1}^{N_g}\sum_{j=1}^{N_g} P(i,j)^2$$	0.24
Correlation	$$Correlation = \frac{\sum_i\sum_j(i,j)P(i,j)-\mu_x\mu_y)}{\sigma_x\sigma_y}$$	0.27
Fractal Dimension	$$Fractal\ dimension\ (D) = \frac{\log(N_r)}{\log(\frac{1}{r})}$$	0.17

Mean Textural Analysis has shown good results for classification of soil and urban classes on the basis of Separability Index as shown in Table 4.11. Soil and Urban class have been classified on the basis of Mean textural Analysis having a threshold value of 19.10 i.e. class is urban when mean value is greater than threshold value and class is soil when mean value is less than threshold value.
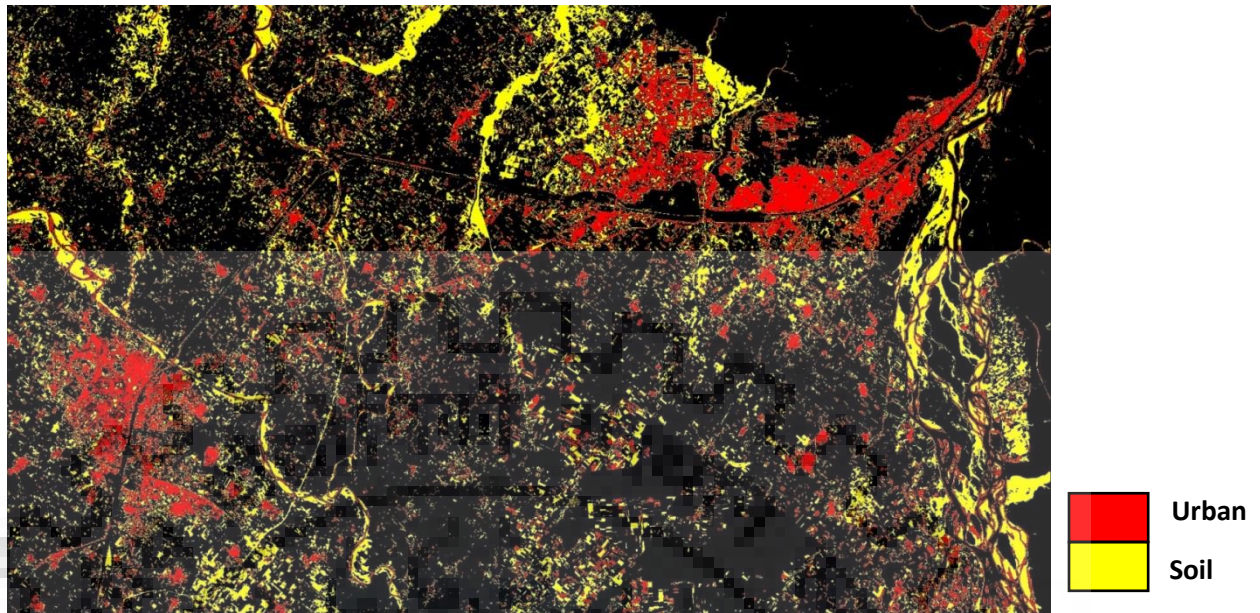
Figure 4.29 Mean textural Analysis (Data Id No. 4)

Accuracy Assessment

Overall Accuracy= 96.28%
Kappa Coefficient= 0.92

Table 4.12 Accuracy assessment for mean textural analysis

| Class	Built-up Area (pixels)	Soil Area (pixels)	Total no. of pixels	Sensitivity	Specificity
Built-up Area	297	29	326	0.983	0.952
Soil Area	5	584	589	0.952	0.983

Soil and urban classification in the image is done using various built-up and radiometric indices. BAEI index has shown the better results than other indices having accuracy of 93.85% with Separability Index of 1.46. To improve the classification results textural analysis has been applied. Second order Mean has improved the accuracy of BAEI classified image to 96.28% with Separability Index of 1.51.

4.5.3 Comparison analysis for Soil and Urban classification

A Sentinel-2 image is taken of date 22 October 2017 and various classification methods are applied. The results of Maximum likelihood classified image are compared with BAEI classified image and Mean textural image. The results shows that previously in Maximum likelihood classified (91.85% accuracy) image lot of urban area has been shown when it is mostly soil. Accuracy of classification is improved by using indexed image such as BAEI index (92.86%).and using mean textural analysis(96.28%).
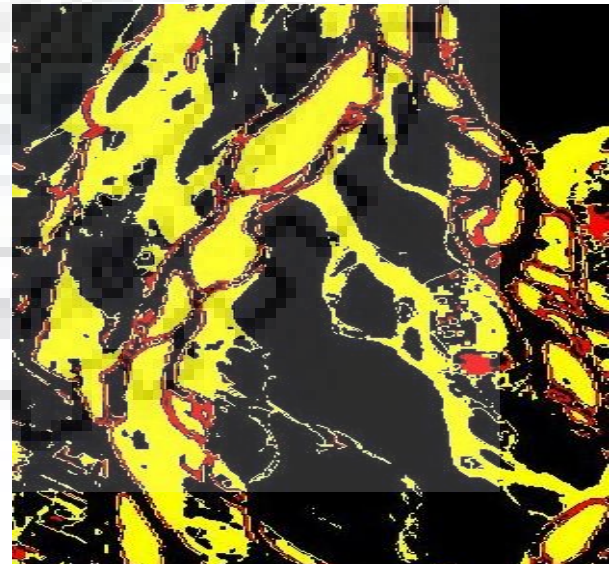

A)
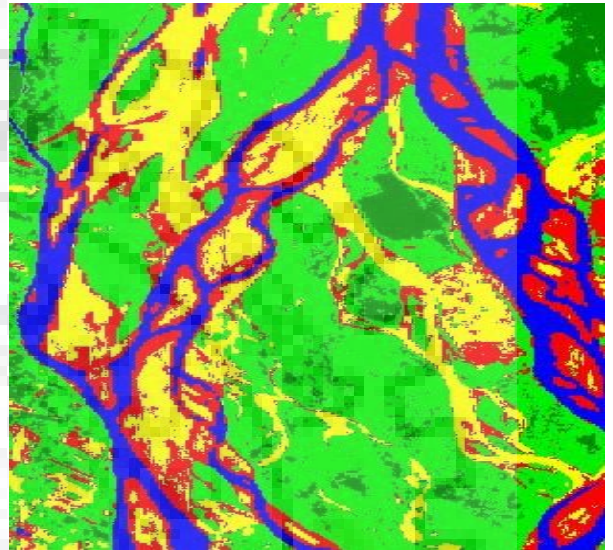
B)
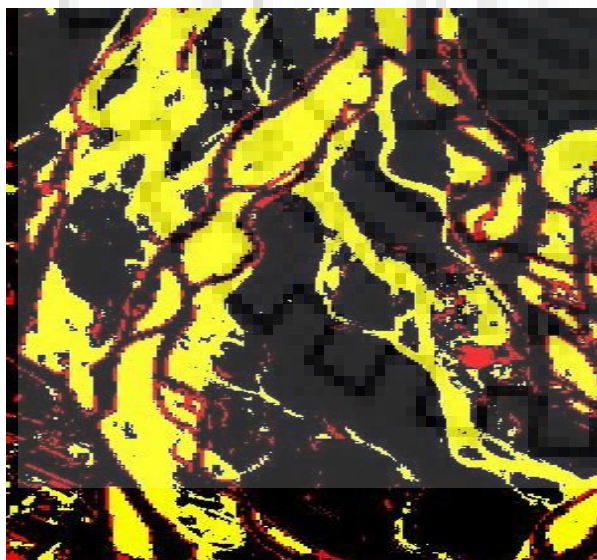
C)

D)

Figure 4.30 A) Seninel-2 image, B) Maximum likelihood image, C) BAEI classified image, D) Mean textural classified image

4.6 Fractional Vegetation Cover using Spectral Mixture Analysis

Fractional Vegetation cover calculation has been explained in section 3.7. After proper classification of image into their respective classes there is need for calculating the vegetation cover within pixels to resolve the mixed pixel issue. For doing this, mainly two classes have been considered i.e. vegetation and soil and linear spectral mixture analysis model has been applied so that proper area of vegetation can be calculated.

Table 4. 13 Reflectance Value of Different Bands

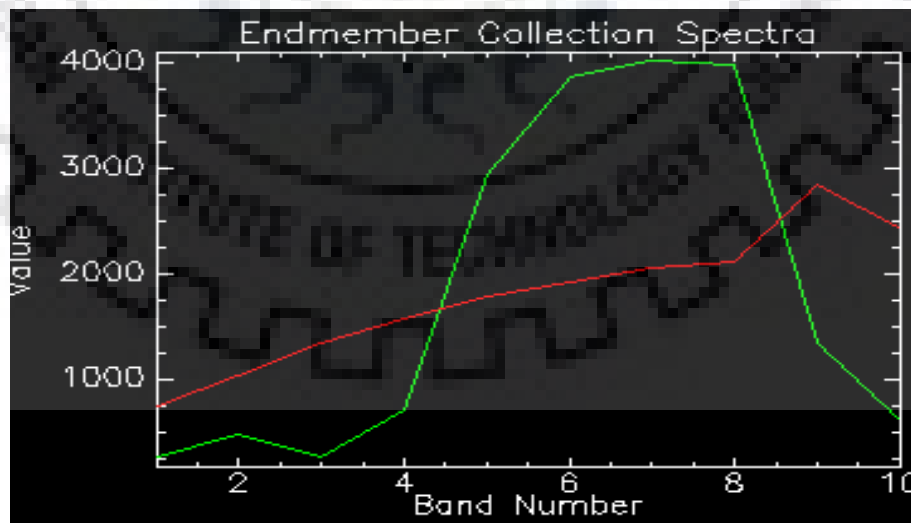| Band Number	Vegetation	Soil
1	0.0294	0.0738
2	0.0512	0.1031
3	0.0356	0.1340
4	0.0784	0.1575
5	0.2150	0.1784
6	0.2609	0.1928
7	0.2724	0.2056
8	0.2737	0.2109
9	0.1316	0.2836
10	0.0719	0.2434

Figure 4.31 Spectral reflectance curve of soil and vegetation

Figure 4.32 Sentinel- 2 RGB (Red- Band 4, Green-Band 3, Blue- Band2) image (14 February 2018)
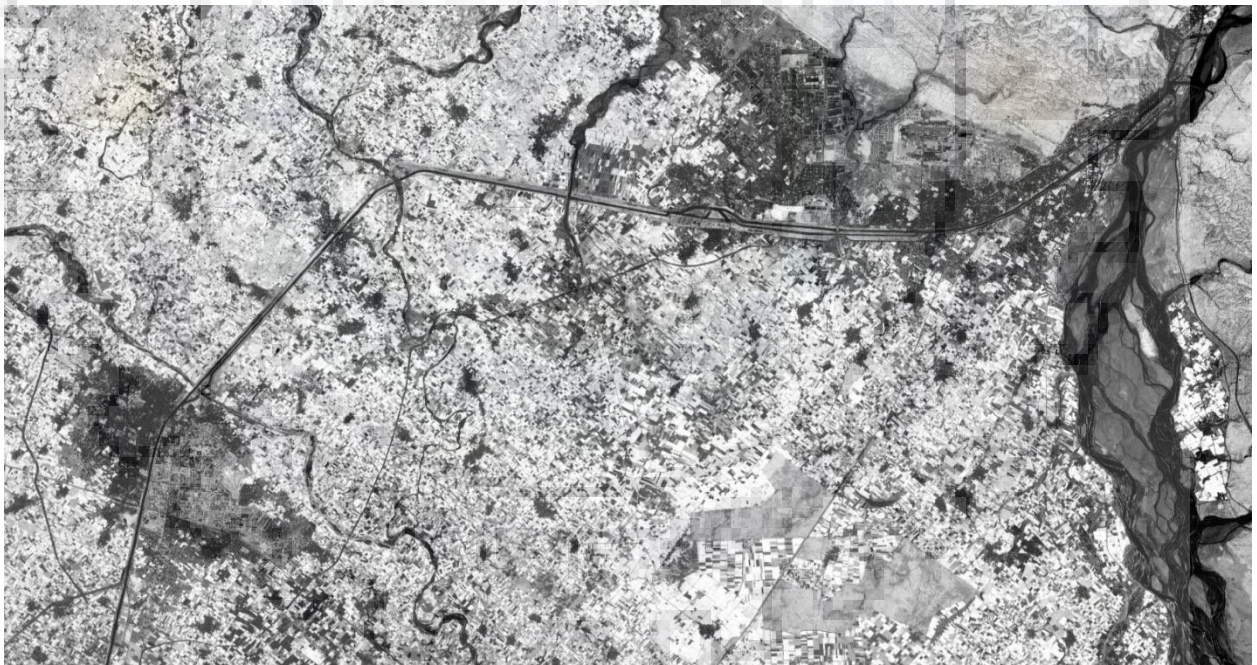

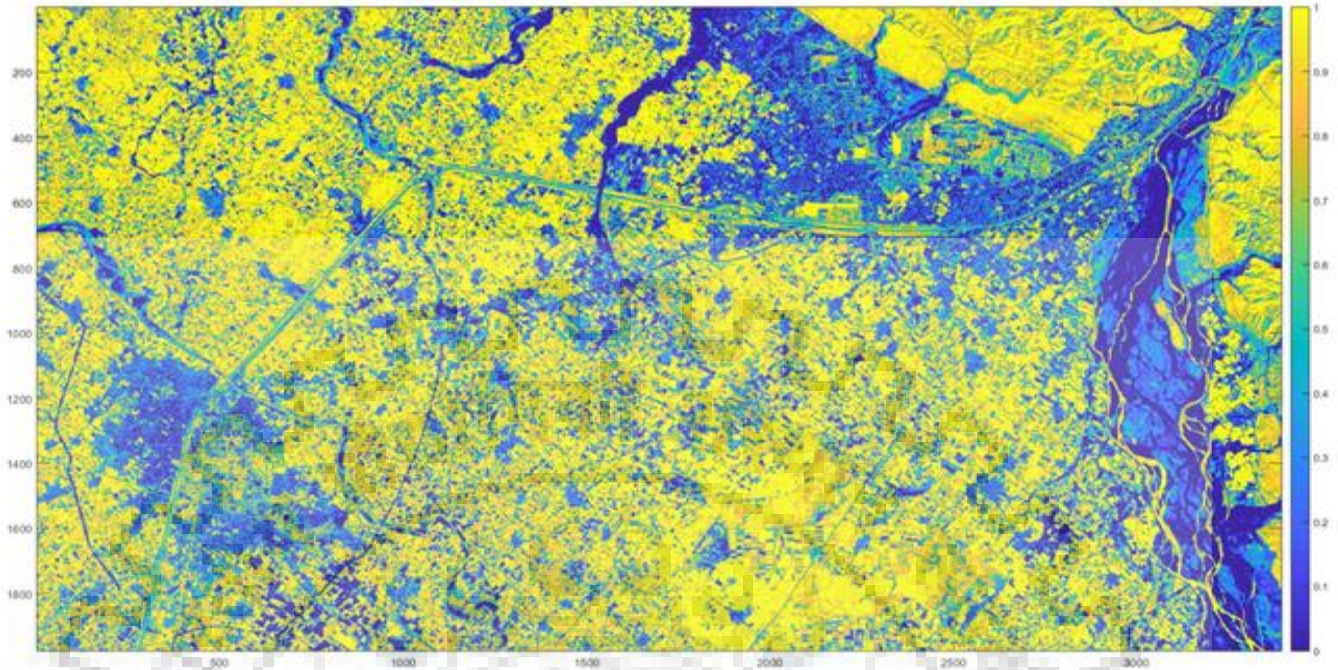**Figure 4.33 NDVI image of Seninel-2**

Figure 4.34 Fractional Vegetation Cover of the image

Vegetation Area Calculation

- Scale(0-1): $f_v = 0$ means zero vegetation in that pixel (blue)

       $f_v = 1$ means full vegetation in that pixel (yellow)

- Total Area of image= 670.6 square kilometers

- Vegetation Area covered= 418.4 square kilometers

CHAPTER 5

CONCLUSION AND FUTURE SCOPE

The present developed system employs several image processing and machine learning techniques to high resolution satellite data for providing solutions of classification techniques for various classes on satellite images namely water, land, urban, forest and vegetation. Apart from using different methods for estimating the area of different land covers, this thesis gives a good knowledge about the processing of mixed pixels. The mostly used method is the analytic solution of the (statistical) linear mixture model when provided with certain class characteristics using the endmember distributions. By the help of linear mixture model, Fractional Vegetation cover has been calculated using spectral mixture analysis by considering two classes namely soil and vegetation. Methods on the basis of indices are fast and simple to execute, their efficiency can change that depends on the characteristics of the sensor along with difficulties inherent to such methods, our main aim is classification between bare soil and urban area. Furthermore statistical textural features such as second order co-occurrence parameters (Mean, variance, Second moment, Entropy etc.) have been applied to classify the soil and urban classes which were becoming inseparable on the basis of spectral features. The comparison is done between supervised learning technique, Indexed method and using Textural features for classification of soil and urban classes. It can be concluded that using indices has improved the classification accuracy to 91.85% from different supervised classification techniques which is having accuracy of 92.86%. Furthermore indexed results have been improved by using textural features which is classifying with accuracy 96.28%.

This work can be extended by map making and map updating data which are the two most important areas, as the requirement for information retrieval, indexing and identification from the satellite images is playing a major role. Crop health monitoring can also be done by using satellite data which is less cumbersome task than doing it manually.

REFERENCES

[1]   J.A. Richards, "Remote Sensing Digital Image Analysis", second ed.,Springer-Verlag, New York, 1993.

[2]   Sunitha Abburu and Suresh Babu Golla, "Satellite Image Classification methods and Techniques: A Review", International Journal of Computer Applications, vol. 119 No.8, June 2015.

[3]   Parker, J.R.: 'Rank and response combination from confusion matrix data', Inf. Fusion, 2001, 2, pp. 113–120

[4]   M. C. Dobson and F. T. Ulaby, "Preliminaly Evaluation of the SIR-B response to soil moisture, surface roughness, and crop canopy cover,"IEEE Trans. Geosci. Remote Sens., vol. GRS-24, no. 4, pp. 517–526,Jul. 1986.

[5]   Xiao yang Tan, Song can Chen and Zhi-zhou, "Recognizing partially. Occluded Expression Variant Faces from Single Training Image per Person with SOM & soft K-NN Ensemble," IEEE Trans. Pattern Anal.vol.16, No. k4, pp.875-855, July 2005.

[6]   G. H. Ball, D. J. Hall, "Iodata A Novel Method of Data Analysis And Pattern Classification", Research Technical Report Stanford Research Institute, 1965

[7]   M.S. Klein Gebbinck and T.E. Schouten, "Decomposition of Mixed Pixels," SPIE 2579, 1995, pp. 104–114.

[8]   Erbek, F.S., Ozkan, C. and Taberner, M., 2004, Comparison of maximum likelihood classification method with supervised artificial neural network algorithms for land use activities. International Journal of Remote Sensing, 25, pp. 1733–1748.

[9]   T. Pant, D. Singh, and T. Srivastava, "Application of fractal parameters for unsupervised classification of SAR images: A simulation based study," in Proc. 1st Int. Conf. Intell. Interact. Technol. Multimedia, New York, NY, USA, 2010, pp. 45–50.

[10] D. Long and V. P. Singh, "An entropy-based multispectral image classification algorithm," IEEE Trans. Geosci. Remote Sens., vol. 51, no. 12, pp. 5225–5238, Dec. 2013.

[11] G. Gutman and A. Ignatov, "The derivation of the green vegetation fraction from NOAA/AVHRR data for use in numerical weather prediction models," Int. J. Remote Sens., vol. 19, no. 8, pp. 1533–1543, Jan. 1998.

[12] B. Johnson, R. Tateishi, and T. Kobayashi, "Remote sensing of fractional green vegetation cover using spatially-interpolated endmembers," RemoteSens., vol. 4, no. 9, pp. 2619–2634, Sep. 2012.

[13] N. Quarmbyet al., "Linear mixture modeling applied to AVHRR data for crop area estimation," Int. J. Remote Sens., vol. 13, no. 3, pp. 415–425,Feb. 1992.

[14] D. Maktav, F. S. Erbek, and C. Jurgens, "Remote sensing of urban areas," Int. J. Remote Sens. 26, 655–659 (2005).

[15] R. B. Thapa and Y. Murayama, "Urban mapping, accuracy, and image classification: a comparison of multiple approaches in Tsukuba city, Japan," Appl. Geogr. 29, 135–144 (2009).

[16] U. Heiden, K. Segl, S. Roessner, and H. Kaufmann, "Determination of robust spectral features for identification of urban surface materials in hyperspectral remote sensing data," Remote Sens. Environ. 111, 537–552 (2007).

[17] D. Lu, E. Moran, and S. Hetrick, "Detection of impervious surface change with multi temporal Landsat images in an urban-rural frontier," ISPRS J. Photogramm. Remote Sens. 66, 298–306 (2011).

[18] Z. Shao, Y. Tian, and X. Shen, "BASI: a new index to extract built-up areas from high-resolution remote sensing images by visual attention model," Remote Sens.Lett. 5, 305–314 (2014).

[19] G. Sun, X. Chen, X. Jia, Y. Yao, and Z. Wang, "Combinational build-up index (CBI) for effective impervious surface mapping in urban areas," IEEE J. Sel. Top. Appl. Earth Observ. Remote Sens., 9, 2081–2092 (2016).

[20] E. Mandanici and G. Bitelli, "Preliminary Comparison ofSentinel-2 and Landsat 8 Imagery for a Combined Use," Remote Sens., vol. 8, no. 12, pp. 1014, 2016.

[21] R. Richter, "Atmospheric / Topographic Correction for Satellite Imagery (ATCOR - 2/3 User Guide)," ATCOR-2/3 User Guid. Version 6.3, pp. 1–71, 2007.

[22] H. van der Werff and F. van der Meer, "Sentinel-2A MSIand Landsat 8 OLI provide data continuity for geological remote sensing," Remote Sens., vol. 8, no. 11, pp. 8832016.

[23] S. Ghosh, S. K. Dubey, "Comparative Analysis of K-Means and Fuzzy C-Means Algorithm", International Journal of Advenced Computer Science and Applications, vol. 4, pp. 35-39, 2013.

[24] Tso, B., Mather, P. M., Classification methods for remotely sensed data, New York: McGraw-Hill, Taylor and Francis, 2001.

[25] G.M. Foody. and D.P. Cox, "Sub-Pixel Land Cover Composition Estimation Using a Linear Mixture Model and Fuzzy Membership Model and Fuzzy Membership Functions," Int. J. Remote Sens. 15 (3), 1994, pp. 619–631.

[26] C.C. Borel and S.A.W. Gerstl, "Nonlinear Spectral Mixing Models for Vegetative and Soil Surfaces," Remote Sens. Environ. vol. 47 (3), 1994, pp. 403–416.

[27] Congalton, R. G., 1991, A review of assessing the accuracy of classifications of remotely sensed data, Remote Sensing of Environment, 37,35–46.

[28] Foody, G. M., McCulloch, M. B., and Yates, W. B., "The Effect of Training Set and Composition on Neural Network Classification", International Journal of Remote Sensing, 1995, vol. 16 (9), pp. 1707 –1723.

[29] M. Herold, J. Scepan, and K. C. Clarke, "The use of remote sensing and landscape metrics to describe structures and changes in urban land uses," Environ. Plann. A 34, 1443–1458 (2002).

[30] S. Sitchet al., "Evaluation of ecosystem dynamics, plant geography and terrestrial carbon cycling in the LPJ dynamic global vegetation model," Global Change Biol., vol. 9, no. 2, pp. 161–185, Feb. 2003.

[31] R. Morgan et al., "The European Soil Erosion Model (EUROSEM): A dynamic approach for predicting sediment transport from fields and small catchments," Earth Surf. Processes van Deventer, A.P.; Ward, A.D.; Gowda, P.H.; Lyon, J.G. Using Thematic Mapper Data to Identify Contrasting Soil Plains and Tillage Practices. Photogramm. Eng. Remote Sens. 1997, 63, 87–93.

[32] M. M. Waqar, J. F. Mirza, R. Mumtaz, and E. Hussain, "Development of new indices for extraction of built-up area & bare soil from Landsat data," Open Access Sci. Rep. 1, 2–4 (2012).

[33] J.B. Campbell. Introduction to remote sensing. Taylor & Francis Ltd, London, 2nd edition, 1996.

[34] Richards, J .A. Remote sensing digital image analysis: An introduction, Springer-Verlag, Berlin, 1986.

thesis